Online Diagnosis of PEM Fuel Cell by Fuzzy C-means clustering

Damien Chanal, Nadia Yousfi Steiner, Raffaele Petrone*, Didier Chamagne, Marie-Cécile Péra
FEMTO-ST Institute, FCLAB, Univ. Bourgogne Franche-Comté, CNRS, Belfort, France

damien.chanal@femto-st.fr ;
nadia.steiner@univ-fcomte.fr ;
**Current affiliation : LUSAC Laboratory (EA4253), Caen Normandy University, 50100, Cherbourg-en-Cotentin, France. ; email address : raffaele.petrone@unicaen.fr*
didier.chamagne@univ-fcomte.fr
marie-cecile.pera@univ-fcomte.fr ;

Keywords

Clustering; Diagnosis; Electrochemical Impedance Spectroscopy (EIS); Fuel cells; Fuzzy C-Means; Non model-based; Proton Exchange Membrane (PEM); Poisoning; Starvation; Water management.

Abstract

To improve the performance and lifetime of Low Temperature Polymer Electrolyte Membrane Fuel Cell (LT-PEMFC), a good monitoring is necessary to detect and recover faults. In this paper an online diagnosis method able to detect the most frequently reported faults in LT-PEMFC, namely flooding, drying, starvation and poisoning is proposed. This method is based on the use of the Electrochemical Impedance Spectroscopy (EIS) as a monitoring tool and a fuzzy C-means classifier to automatically identify the faults at an early stage. To validate the proposed methodology and emphasize its genericity, the algorithm has been tested on data extracted from two different stack technologies: one fed with hydrogen and pure oxygen and another one with hydrogen and air. The experimental tests were carried out by two different laboratories using different test benches.

Introduction

Hydrogen is one of the main candidates as an energy carrier the future of clean energy. Thanks to the ability to produce it by electrolysis from renewable energies, its high energetic potential and its suitability as a fuel for fuel cells, the interest in hydrogen increases strongly. Currently, Low Temperature Proton Exchange Fuel Cell (PEMFC) is the most mature technology. The principle of PEMFC is to produce water, heat and electricity from an oxidation-reduction reaction of hydrogen and oxygen. Despite a good efficiency (#50% - 50% electrical- thermal), a low operating range temperature (0 – 80 °C) and low pollution (waste is the produced water), PEMFC still suffer from a too high cost and short lifetime. In addition, even if it is possible to produce hydrogen by water electrolysis, currently 96% of the hydrogen produced comes from the reforming of natural gas (HJ, 2019). One of the objectives of the Department Of Energy (DOE) is to increase lifetime of fuel cells for stationary and transportation up to 40 000 and 5 000 hours respectively under realistic operating conditions (“Fuel Cells,” n.d.). Realistic operating conditions include impurities in the air, startup and shutdown, but also freezing and many other conditions that affect fuel cell operation. (membrane degradations, corrosion of catalyst …). These faults can impact fuel cells by degrading internal components such as the PEMFC membrane or corroding the catalyst ... but can also damage the entire system.

One of the keys to increase the lifetime of PEM is an early detection of faulty operating conditions and the implementation of mitigation strategies to avoid irreversible degradations. The objective of diagnosis is to regularly assess the state of health of the fuel cells in order to detect a fault as soon as practicable. Currently, there are many diagnostic methods using different approaches to detect faults in systems (Lin et al., 2019; Petrone et al., 2013; Zheng et al., 2013).

This paper presents a method of diagnosis developed during the European project HEALTH CODE ("Real operation pem fuel cells HEALTH-state monitoring and diagnosis based on dc-dc COnverter embeddeD Eis," n.d.) and continued by the European project RUBY ("RUBY – EU project," n.d.) whose objective is to design and realize an embedded Monitoring, Diagnostic, Prognostic and Control (MDPC) tool. The monitoring tool developed during HEALTH CODE project permits to measure the Electrochemical Impedance Spectrum in PEMFC online, based on a relevant control of the DC/DC converter. The acquisition of the electrochemical impedance spectrum is then possible online with a low additional cost. The description of the modified DC/DC converter is beyond the scope of this article. EIS can be used as a monitoring tool because several phenomena occurring in the fuel cells are sensitive to the solicitation frequency and then have a characteristic signature on the Nyquist and Bode diagrams. Diagnostic and monitoring tools have been tested on two stacks: a hydrogen - oxygen stack and a hydrogen - air stack. Experimental tests were carried out by two different laboratories using different test benches.

In the first section, a state of the art of different existing diagnostic methods is introduced. In the second section, a presentation of diagnostic algorithms developed is proposed. The third section is devoted to the explanation of the experimental trials carried out on both stacks as well as the presentation of the collected data. Finally, a presentation of result and the discussion about the designed algorithm is done in section 4.

1 State of the art of PEM fuel cell diagnostic methods and Fault monitoring

Currently, one of the limitations to the democratization of fuel cells is their short lifetime. Beyond the technological aspect (materials of components, design and stack assembly), a good diagnostic algorithm should be present to improve performance and increase the lifetime of fuel cells. Diagnosis is useful to detect and identify abnormal conditions such as for example contamination, starvation and water management dysfunctions (Giurgea et al., 2013; Hinaje et al., 2009; Li et al., 2008; Taniguchi et al., 2008; Yousfi-Steiner et al., 2009, 2008). In this section a brief presentation of main fault detection and identification (FDI) methods is done to introduce the chosen method in section 3.

Two approaches to detect and identify faults in fuel cells exist: "model-based" and "non model-based".

The first type (i.e. model-based) needs a deeper understanding of the studied system. In case of black box-models, an analytical model referred to a database. Measurements on the real system are then compared to the model outputs, given the same inputs: residuals are analyzed, and gaps are interpreted as symptoms of an occurring fault.

Non model-based methods can be signal-based, data-based or knowledge-based type. This model is executed in two steps: an offline step where the algorithms learn with known data (faults associated with each data are known) and an online step where the new data is classified into classes learned offline to give the SoH of the system. Non-model-based approaches is used to obtain information and determine state of health of fuel cells by using heuristic knowledge and/or signal processing to determine the state of health of fuel cells. In (Mouzakitis, 2013), an overview of several methods of classification for control systems is given, while a recent review on hydrogen fuel cell fault diagnosis and prognostic methods is made in (Lin et al., 2019). The thesis in references (Li, 2014) presents several diagnosis approaches. In Figure 1, a global presentation of main diagnostic families for fuel cells is proposed, this figure will be detailed below.

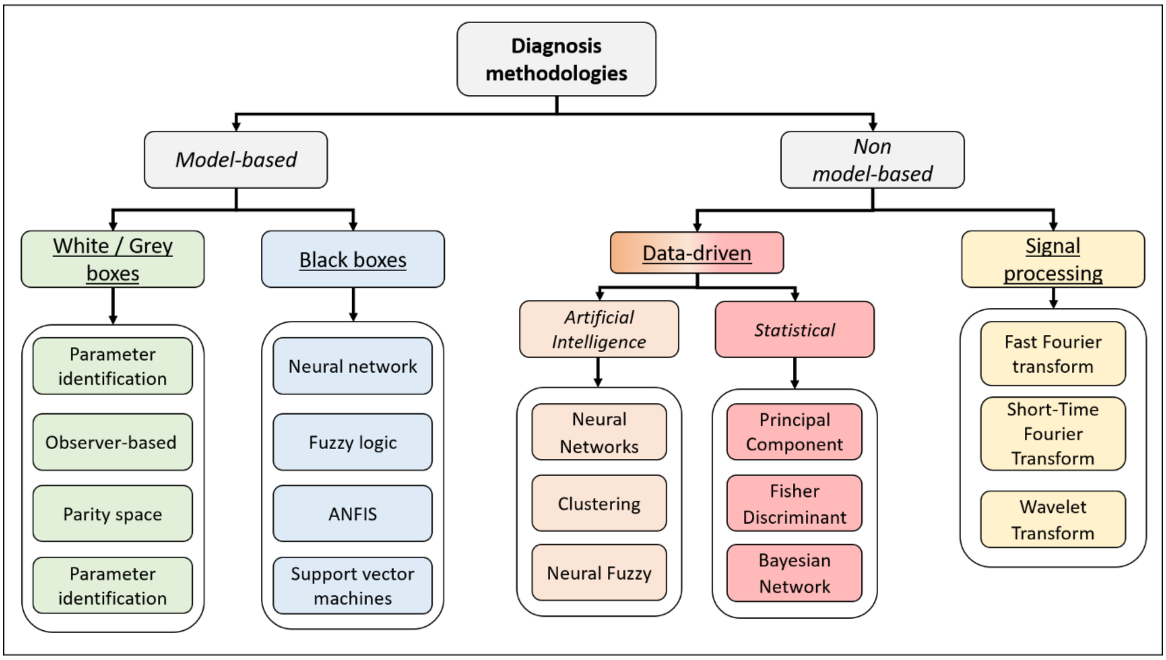

Figure 1 : Presentation of the main families used for fuel cell diagnostics

1.1 Model-based approaches

1.1.1 Generalities

As explained previously, model-based diagnostic measure outputs given by a functioning system and a model with the same inputs. Residuals between these both outputs are analyzed and it permits to determine the SoH of the analyzed system. Figure 2 shows the principle of model-based diagnosis:

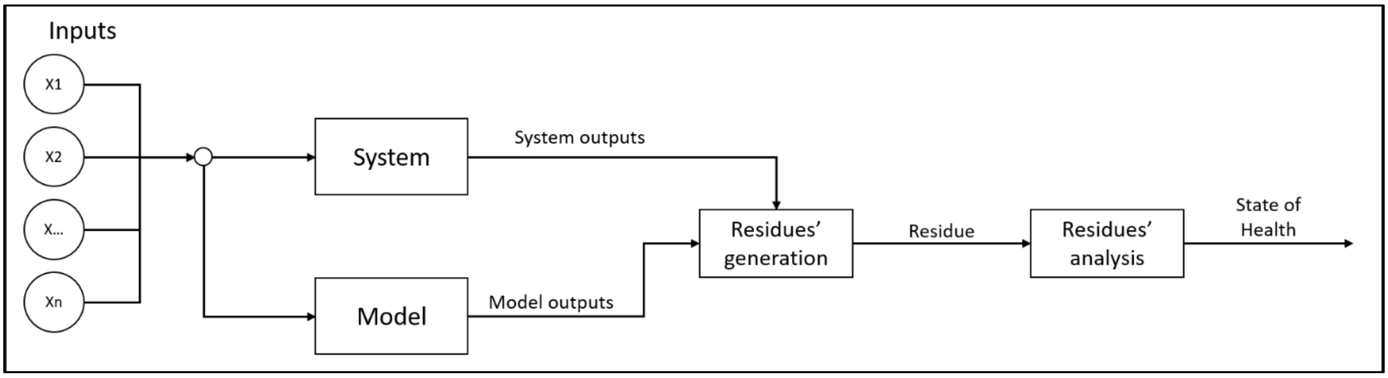

Figure 2 : Principle of model-based diagnosis

The main difficulties generated by the model-based approach are: the definition of normal and abnormal operating thresholds, the generation of enough residuals to isolate a fault which may require a large number of sensors. Moreover, the reliability of the model is the crucial point of this approach. In order to optimize model-based algorithms, different types of methods have been developed. Each has its strengths and weaknesses even though they all follow the same basic principles. The following section details several types of model-based methodologies.

1.1.2 Details on model-based approaches

Three types of model based diagnosis can be found in the literature: "white box", "black box" and "grey box" (Ding, 2008; Petrone et al., 2013).

The first type called "white box" uses algebraic and/or differential equations to describe phenomena occurring in fuel cells system. In the case of PEMFC modelling, the most used physical laws are Nernst, Planck, Butler-Volmer and Fick's which reproduced the charge transports and mass transfers phenomena. In (Bernardi and Verbrugge, 1991) a macro homogeneous description of a membrane air-fed and the predicted polarization are compared with experimental results.

The main advantage of white box models is their accuracy. However, these models can be difficult to implement online and the complexity of the calculations leads to a high computational time. They often need to have internal information on the know-how of the stack supplier and stack design that are not always available.

To replace some mathematical complex equations in white box models, a second type named "Grey box" was developed. This model replaces some physical laws by empirical formula or map tables. Main different approaches are defined below:

- Parameter identification models

The principle of parameter identification models relies on the fact that either components or physical phenomena are correlated with a nominal condition. Faults conditions are defined as system parameters. When parameters reach a certain limit, the correlation fault can be detected and isolated. One example of a parameter identification model is developed in (Rubio et al., 2007) where a correlation between the value of the diffusion layer resistance and the water content in the fuel cell was found. This model uses an equivalent circuit to calculate some relevant PEMFC parameters.

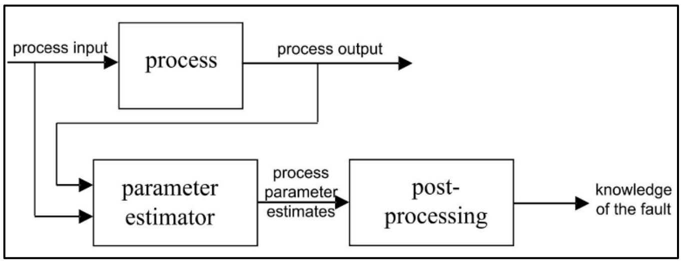

Figure 3 : Schematic description of parameter identification scheme (Ding, 2008)

- Observer-based models

Observer models are based on mathematical equations to describe the system's behavior. A model is implemented with the system and runs in parallel with it. This method uses an observer to generate residuals between the measured value of the system and the value obtained from the observer. It is the one of the most common approaches implemented for model-based diagnosis. Main of these models focus on state estimation without any diagnostic phase. FDI is done by an analysis of residuals. Model-based observer are divided into several categories : Kalman filter, Luenberger and sliding mode observers (Yuan et al., 2020).

Kalman filter is a recursive filter which estimates internal state of a linear dynamic system (i.e. minimum mean square error) from noisy measurements acquired at discrete real-time periods. (Bressel et al., 2016) presented an Extended Kalman Filter to estimate the State of Health of a PEMFC.

The Luenberger observer compares the measurable and estimated quantities of the system. It provides a convergent error dynamic through the feedback gain. (De Lira et al., 2009) used a linear parameter variation observer (LPV) with Luenberger structure is applied for the calculation of the residuals. This methodology allows linearizing the system equations and solve the analytical problem in a discrete time state space.

Based on the control theory of the sliding mode variable structure, the sliding mode observer directs the dynamic response of the system in a continuous and targeted manner to follow the predefined trajectory and finally converge close to the surface of the predefined sliding mode to reconstruct the system states. (Liu et al., 2016) developed a nonlinear observer-based fault diagnosis approach for PEMFC. Model used to design the observer is a modified super-twisting sliding mode algorithm.

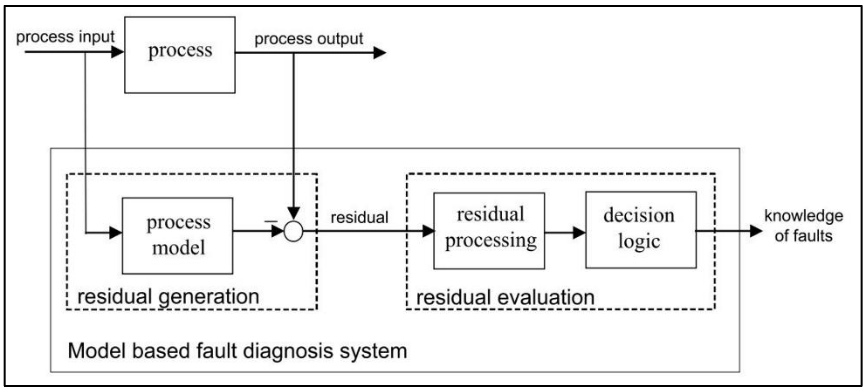

Figure 4 : Schematic description of the model-based fault diagnosis scheme (Ding, 2008)

- Parity space methods

Parity space methods adopt parity relations (i.e. the redundant relationship between variables) instead of an observer to generate residuals. In the FDI parity space, the generation of residuals, the dynamics of residual signals concerning defects and unknown inputs are presented as algebraic equations. The parity space method is based on the verification of the static relationship between the different measurements in the time window. (Hamaz, 2014) defined a parity space as the orthogonal of the observability matrix. This method avoids the influence of state on the system. (Petrone et al., 2013) presented parity space as a useful method to linearize a system in a discrete subspace. This allows simplifying the computational cost.

The main advantages of grey boxes are their calculation time and their simplification of the equations compared to white boxes. Nevertheless, these models require knowledge (like for white boxes) and the identification of the parameters in the grey boxes can require a significant numerical effort.

Last type of model-based diagnosis is called “black box”. With this model, relationship between inputs and outputs are based on statistical data-driven approaches and not physical laws. Contrary to white box models, black box models are directly derived from experiments and are mainly used for complex system as fuel cells. A specification for black boxes models is the necessity to know the class of each data to create a link between input (data) and output (class). Different approaches for black box models are described below:

- Artificial Neural Networks (ANN)

Artificial Neural Networks (ANN) are models inspired by the functioning of animal brains. With data given as input, neurons models build in two steps a non-linear mapping of the system. First, each input is weighted and added, then result is used as argument of a function f (linear or non-linear). (Jemeï et al., 2003) propose an Matlab/Simulink ANN model to describe a proton exchange membrane fuel cell (PEMFC) integrated to a complete vehicle powertrain.

- Fuzzy logic (FL)

Fuzzy logic can be very powerful to describe complex systems, mainly with ambiguities and non-linearities. FL tends to represent the human reflection by combining: IF – THEN rules and logical operators AND – OR, with the objective to convert numeric value to fuzzy set (Fuzzification process). Thanks to “if – then” rules, a membership is assigned to each fuzzy set converted in numerical value (Defuzzification process). (Hissel et al., 2004) proposed a diagnosis model of PEMFC using fuzzy logic to detect water management problems.

- Adaptive neuro-fuzzy inference systems (ANFIS)

ANFIS model is a good mix between ANN and Fuzzy Inference System (FIS). FIS is the process of formulating the mapping from a given input to an output using fuzzy logic. ANFIS combines human like reasoning with the connectionist structure of artificial neural networks. This method is interesting for the diagnosis domain because it contains advantages of ANN and FL. In (Kaid et al., 2018) a diagnosis model based on ANFIS is used to detect failures in photovoltaic system. In (Sanchez, 2015), a method based on ANFIS is developed for the prognostic of fuel cells.

- Support vector machines (SVM)

  Another black box model is the Support vector machines SVM. This method is based on statistical learning theories. SVM concept is to map non-linear data into a high dimensional space (i.e. feature space) and then to use process to linear regression to perform the model. The reference (Li et al., 2016) presents a diagnosis model using SVM as a fault classifier for PEMFC systems.

The main advantage of black box models is their efficiency with complex and non-linear system such as fuel cells. However, to be effective, it needs a large database, which is not always possible.

1.2 Non model-based approaches

1.2.1 Generalities

In the field of diagnosis, to describe non-linear and multi fault system, it could be complicated to develop models based on the knowledge of a system. Due to this reason, the use of data driven methods and signal processing have been developed. Non model-based approaches process in two times: Firstly, the algorithm is trained with known data (off-line/training) and then it processes on-line with a new data using information from the training.
Off-line section is composed of several steps. As a first step, it is important to obtain a large database with quality data. This step is important because methods that do not rely on models can only classify cases that they have encountered during offline learning. The database is expected to be as complete as possible and without biases. The database is therefore the heart of this methodology. The second step is the extraction of data from the experiments. Indeed, it may be necessary to extract interesting features from the acquired data (this is notably the case for signals). Thirdly, the features are standardized to put them all at the same scale and limit the influence of some of them in relation to the others. The next step is to select the most interesting features : the number of features has to be as small as possible to reduce the computation time and each feature should carry as much and independent information as possible in order to improve the quality of the results. The last step is to teach the algorithm how to classify the known data in order to have clusters in the features' space able to represent the different states of health of the system.

In the on-line part, a new measurement is acquired. Features are extracted and processed to find the features' cluster to which the set belongs, in order to assess the current state of health of the system. The several steps for off-line and on-line section are shown below:

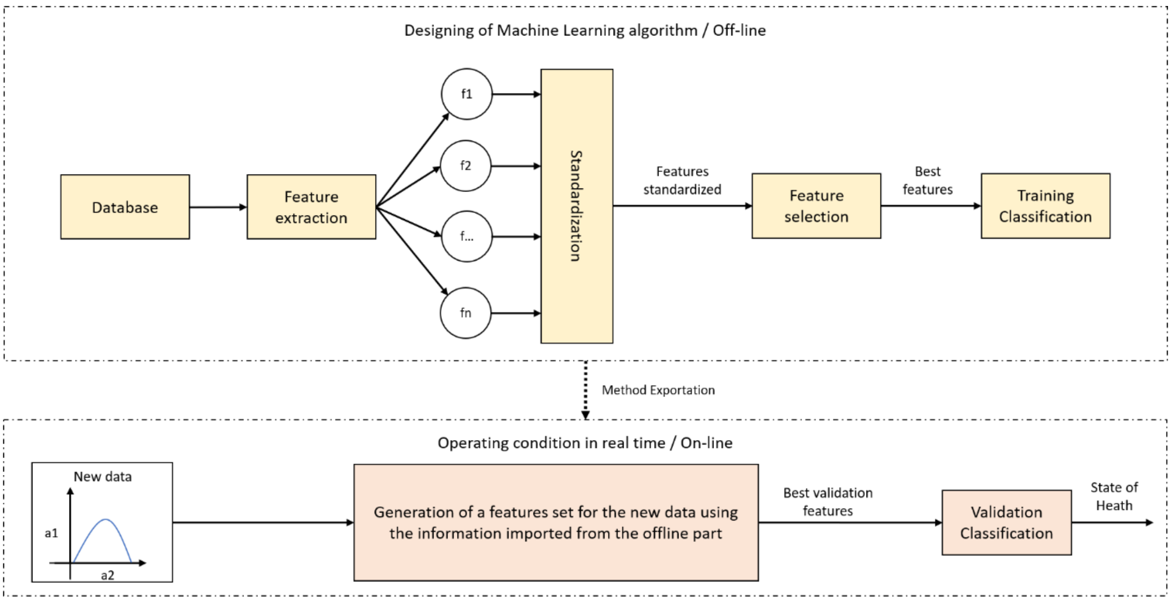

Figure 5 : Principle of non model-based algorithms

The main advantage of non model-based algorithms is their robustness with noisy data compare to model-based which need clean input to function correctly. These models are efficient tools due to their simplicity, flexibility and ability to handle non-linear problems. In addition, these models do not require any knowledge of the system structure. However, these algorithms can only handle situations already encountered during the learning phase.

Non-model-based methods can be divided in three families: Artificial Intelligence, Statistical methods and Signal processing (Zheng et al., 2013). Each of these families is specialized in a field such as feature extraction, selection or classifier. In addition to the state of the art on these methods, comments on the selected methods will be provided in the following sections.

1.2.2 Details on Features Extraction

Signal based models are efficient tools to extract valuable features from a signal, that can be affected by the occurrence of certain types of faults. In general, the oscillations that can be viewed in PEMFC's signals are of harmonic and/or stochastic nature. Signal processing needs two elements to be efficient: the selection of a relevant signal to use for monitoring, and a good signal analysis approach to interpret the obtained data. The known techniques for signal processing are described in this section: Fast Fourier Transform (FFT), Short-Time Fourier Transform (STFT) and Wavelet Transform (WT).

- Fast Fourier transform (FFT) and Short-Time Fourier Transform (STFT)
  The idea behind FFT methods is to convert a stationary signal from a time domain into a frequency domain. The signal is then represented by a magnitude and a phase for each frequency. Thanks to FFT, an original signal can be transformed into a power spectrum. Interest of power spectrum is that significant components can be obtained by an analysis. (Chen and Zhou, 2008) used a FFT to correlate the stack voltage with the pressure drop across the cathode/anode of a PEMFC. The main limitation is that, in real life, signals are not stationary.
  The STFT method is then an upgraded version of FFT which decomposes a signal into a set of small segments with a given window length. This allows assimilating each segment as stationary and then processing to a traditional FFT. In (Yu and Lu, 1994), a discussion about STFT and Wavelet Transform (WT) is made. They have shown that one of the best substitutions of the Gaussian function in the Fourier domain is a square sinusoidal function that can form a biorthogonal window function in the time domain. The merit of a biorthogonal window is that it could simplify the inverse STFT and the inverse WT.

- Wavelet Transform (WT)
  Another option to cope with the analysis of transitory signals is the Wavelet Transform WT. This method is useful to mix time and frequency resolution. The basic idea of WT is to represent any function as a superposition of a set of wavelets. This method can be performed by several types of wavelets. Unlike in STFT, WT uses an adjustable size for the window with the frequency of local area: the window is shorter for a high frequency than a low frequency, that permits to have the best trade-off between time and frequency resolution. Two types of WT are mainly found: Continuous Wavelet Transform (CWT) and Discrete Wavelet Transform (DWT). According to (Zheng et al., 2013) CWT is a more efficient method for the time and frequency resolution of signal however DWT needs less time calculation and has a powerful de-noising capability. One crucial point is the selection of wavelet type as developed in (Rafiee and Tse, 2009). In (Pahon et al., 2016) a presentation of a signal-based method using WT is made to detect and identify a high air stoichiometry fault.

Signal-based models are effective tools for detecting and extracting relevant characteristics of the signal provided by fuel cells, such as polarization curves and electrochemical impedance spectra. However, signal based are not used in the designed algorithm. The monitoring by EIS is a well-known methodology and significant features can be found in literature (this part is described in section 2.2) has been preferred.

1.2.3 Details on Standardization methods

Standardization consists in transforming data form when they are not in the same range to eliminate distortions of the SoH space. Magnitude of features can affect algorithms, especially when some features have much larger values than others. This leads to distortion and can thus diminish or make the information contained in the others disappear.

Outliers and noisy data are the best example to illustrate the importance of standardization. Therefore, it is important to select the most suitable method to standardize data in the most usable and efficient form according to the dataset.

For the purpose of this document, the algorithms have been developed in a Python environment using the Sklearn (Pedregosa et al., 2011) and Scikit-Fuzzy (Josh Warner et al., 2019) libraries. Six methods to standardize data are presented in Table 1:

Table 1 : Main standardization method in Machine Learning (sklearn distribution)

Type of transformation	Method	Principle
Linear	Min-Max Scaler	Scale each feature in the range [0 – 1]
	Standard Scaler	Scale features by removing the mean and scaling to unit variance
	Robust Scaler	Scale features by removing the median and scaling according to the quantile range.
Non-Linear	Quantile Transformer	Transform features to follow a uniform or normal distribution using quantiles information
	Power Transformer	Transform features to make data more Gaussian-like
-	Normalization	Scale individual samples to have unit norm

Min-Max Scaler and Standard Scaler are two powerful standardization methods; however, they are very weak to cope with outliers. For that reason, the Robust Scaler was developed. It uses statistics to reduce the importance of outliers. Normalization scales samples and not features to have a unit norm. Non-linear transformations are based on monotonic transformation that permits to preserve the rank of values along each feature. They are very powerful with outliers. In the design step of the algorithm, all these methods were tested and it has led to select the "Quantile Transformer" which transform features to follow a uniform distribution. The comparison between standardization methods is not presented in this document.

1.2.4 Details on Features Selection

Statistics methods are mainly used as variable dimension-reduction methods which are needed to find relevant feature in Artificial Intelligence algorithms as explained previously. Usually, a lot of features are used in data-driven models but only a few of them contain real important information. Most of the database size reduction methods used are Principal Component Analysis (PCA) and Fisher's Discriminant Analysis (FDA) but these methods assume there is a linear correlation between features. Other method to reduce database size is based on the use of Correlation Coefficients and statistical test such as F-Test and Mutual Information.

- Principal Components analysis (PCA)

  PCA is the most common dimensionality reduction method. With this method, correlated variables are converted into uncorrelated principal components which permit to save the largest variance among features. In (Zhao et al., 2017) a fault classifier based on multi-sensor signals and using PCA method is used for the diagnosis of a PEMFC. The main advantage of PCA is that it improves results by reducing the number of correlated features (too many can create an overfitting phenomenon) without needing the label of data. It is an unsupervised dimensionality reduction method. A reduced number of correlated features not only accelerates the computer's calculation speed but also improves the visualization of results in 2D or 3D graphics. However, PCA modifies the basic features into main components (linear combination of the original features) which are more difficult to interpret. One of the constraints of PCA is that it must be used with "Standard Scaling" type standardization (mean = 0 and standard deviation = 1) to obtain optimal performance.

- Fisher Linear Discriminant Analysis (FDA)

FDA is a kind of supervised dimensionality reduction technique. In the case of diagnosis, data obtained from several states of health are collected and categorized in classes. The idea of FDA is to select a set of discriminant vectors by maximizing the scatter between classes and minimizing scatter among each class. In (Gharavian et al., 2013) a comparison between PCA and FDA as feature selector methods is done for faults diagnosis of automobile gearboxes. FDA is a very powerful method for dimensionality reduction when they respect the assumptions that observation is normally distributed and that they share the same covariance matrix. However, FDA is limited in performance in the case of noisy and sparse data.

- Correlations coefficients (Pearson, Spearman & Kendal)

Correlations coefficients are statistical measures to catch relationship between variables. Relationship values are in the range [-1, 1]. The closer the relationship between two variables is to 1 or -1, the closer the correlation between these two variables will be perfectly positive or negative (depending on the sign of the value). There is no correlation between two variables when this value is equal to 0. It is interesting to know the relationships between the different variables for the sake of avoiding the presence of two variables giving the same information. It exists several types of correlations coefficients, but the three mains are: Pearson, Spearman and Kendal.

Pearson product-moment correlation coefficient is the most used coefficient, it consists in the measure of how strong is of the linear correlation between two variables.

Spearman rank correlation coefficient is a non-parametric measure of rank correlation between two variables. It consists in the assess of how well the relationship between two variables can be described by a monotonic function.

Kendall tau rank correlation coefficient is a non-parametric hypothesis test used to measure the ordinal association between two variables.

A comparison between Pearson, Spearman and Kendall Correlation Coefficients is presented in (Chok, 2010)

- ANOVA F-Test

Analysis of variance (ANOVA) is a tool to compare the means of several populations, based on random, independent samples from each population. It provides a statistical test to determine if population means are equal or not (i.e. came from the same distribution). ANOVA is a parametric test that assumes a normal distribution of values (null hypothesis).

F-test is a class of statistical test that calculates the ratio between variances. F-Test is used with ANOVA to measure the ratio between explained and unexplained variances.

Three assumptions must be satisfied with ANOVA F-Test: samples are independents, from normally distributed population and standard deviations of the groups are all equal (homoscedasticity). It permits the measure of the linear dependency between two variables. In (Johnson and Synovec, 2002) a feature selection based on ANOVA and PCA is done to classify jet fuel mixture. In (Yakub et al., 2016), a feature selection based on one way anova is used to classify microarray data. Main advantage of ANOVA F-Test is its straightforward computation and interpretation. The limiting factor is that its applicability is only valid with the specific assumptions.

- Mutual Information

Mutual Information also named information gain is a quantity which measure the mutual dependence (i.e. it quantifies the amount of information) between variables. It is a non-parametric test which significates that it doesn’t require a normal distribution to be analyzed. Contrary to correlation coefficient, mutual information is not limited to linear dependance. Mutual information is null if variables are independent, and it increases as dependency increases. In (Liu et al., 2008) a general criterion function for feature selection using mutual information is proposed. Mutual information are efficient tools to catch statistical dependency but because they are non-parametric, they need more samples to be accurate.

In the designed algorithms, the features selection is based on the use of the Pearson product-moment correlation coefficient to filter redundant information and an ANOVA F-Test to select best features. This method is selected because it mixes both advantages of correlation coefficients and statistical tests. PCC deletes features highly linked and ANOVA F-Test captures the linear relation between features and targets.

1.2.5 *Details on Classifiers*

Classification is the core of non-model-based algorithms. It consists in the creation of relations from a known database to class a new data in a class/pattern. In this section, five classifiers are presented. The first is a classifier based on statistics while all others are based on the use of data and more precisely on Artificial Intelligence.

- Bayesian Networks (BNs)

Bayesian Networks are graphical-probabilistic structures using database to process. They are constructed in two steps: finding networks structure and then calculating conditional probabilities from data. The relationship between the nodes of each layer is a cause and effect relationship that can be quantified by conditional probabilities. In (Riascos et al., 2007) a BN is used for PEMFC diagnosis. A graphical model presenting the cause-effect relationship between features and another probabilistic method captures numerical dependence between variables. BNs are useful robust tools for dealing with diagnosis problem which are uncertainty, the decision and the reasoning. Nevertheless, time compilation can be very slow.

- Artificial Neural Networks (ANNs)

Even if ANN are model-based to generate residue, it is possible to use them a classifier. A famous ANN model working as a non-model-based is the Hamming Neural Network (HNN) which uses pattern recognition to find the closest class. Another possibility is to use the HNNs to determine the age of the fuel cells (Kim et al., 2012). Recently, a proposed brain-inspired computational paradigm called “Reservoir Computing” was developed for fuel cells diagnosis (Zheng et al., 2017). The considered “Reservoir” is made of a particular class of complex dynamics emulating a virtual neural network and modeled by a nonlinear delay equation. Non model based ANNs have the advantage of excellent nonlinear approximation ability, moreover, they are less sensitive to noise than ANN model based. However, non model-based ANNs have need high computation time for the training step. The higher the number of defects to be classified, the larger and more complex the network is. This can lead to a long and difficult training of all defects without significantly increasing performance.

- Neural Fuzzy

Neuro Fuzzy is a combination of human like reasoning of fuzzy system with the structure of ANN. ANFIS is one of the most popular form of neural fuzzy. ANFIS can be used as model-based method but it is also possible to process to pattern recognition. In reference (Escobet et al., 2014) a hybrid model based on fuzzy and pattern recognition techniques is proposed for PEMFC diagnosis. Neural Fuzzy algorithms is a powerful tool which is adapt to noisy data as for fuel cells system. However computational time for the training of ANFIS can be significant.

- K-nearest neighbors (KNN)

KNN is a non-parametric method used for classification. It is also one of the best-known classification algorithms. Principle is that known data are arranged in a space defined by the selected features. When a new data is supplied to the algorithm, the algorithm will compare the classes of the k closest data to determine the class of the new data. In (Medjahed et al., 2013) a study of a KNN algorithms is performed to classify breast cancer. Analysis consists in the observation of the impact of parameters such as distance and classification rules on classification results. The major advantage of the KNN classification is its simplicity, it is also an efficient method. However, despite its efficiency, computation times can be long with large databases, the determination of the number of neighbors to use (k) requires trial and error and the algorithm is weak with outliers which can strongly impact its efficiency.

- Clustering (K-Means / C-Means)

Principle of clustering is to divide unlabeled data into several groups called clusters. In the case of fuel cells diagnosis, cluster could correspond to faults such as flooding or drying at several levels. Two mains algorithms for clustering exist, the hardening K-Means and the C-means clustering (also named Fuzzy K-Means). The difference between hardening and fuzzy clustering is that C-means uses a weighted centroid based on probabilities whereas the membership assigned by the K-Means algorithm only depends on the closest cluster. (Zheng et al., 2014) presented a double-fuzzy diagnosis methodology to detect online fault in PEMFC. Firstly, a fuzzy clustering approach is done before the use of a fuzzy logic approach (rules). (Liu et al., 2018) presented a model to diagnose PEMFC system of tramway based on K-Means clustering. K-Means is used to filter singular sample points, then the Lloyd's method is used to quantify sample vector sets and obtain the discrete code combination of training and test samples. The Baum-Welch algorithm and the backtracking algorithm are respectively adopted to form and infer the DHMM. Clustering methods are effective tools for classifying data. Indeed, they are simple to implement, flexible, and perfectly suited to large databases. Unlike methods that use neural networks, the training phase does not require a large computational cost. However, this method requires a good analysis of the data to determine the most suitable number of clusters. Clustering algorithms proceeding by iterations in order to create clusters can affect the robustness of the algorithm due to local optimizations depending on the cluster initialization. Data standardization has a huge influence on clustering algorithms. Indeed, these algorithms use the distance between points and centers to define the membership. The standardization method and the metrics used to measure the distance between clusters and points are crucial parameters.

The classifier used in this article is fuzzy-C-means. This choice is explained by its simplicity of use and its speed to process large databases contrary to other classifiers which are efficient also but need high computational time. This method is particularly adapted to a real-time diagnostic algorithm.

1.3 Diagnostic tools for PEMFC faults monitoring

In order to be able to observe the degradation of PEMFCs, diagnostic tools have been developed. These tools can be divided in two families: In Situ and Ex Situ. In situ method permits to observe electrochemical variables (voltage, current …) under operating conditions while Ex situ characterizes detailed structure and properties of each component. In this section, a presentation of the main In Situ diagnostic tools is proposed. Other In Situ methods exist such as current mapping, transparent cell or cathode discharge, however they are laboratory methods that are not yet adapted to an on-board commercial application. In addition, Ex Situ methods are not presented in this article because they are not adapted to on-board application.

- Fundamentals of fuel cells

From a thermodynamic point of view, the entire heat released by fuel cells reaction is defined by the enthalpy change ΔH:

$$\Delta H = -n.F.E_T \quad [1]$$

n is the electron transfer number in the reaction (2 for H_2), *F* the Faraday constant (96485 $C.mol^{-1}$) and E_T the theorical voltage if all H_2 energy is consumed to produce electricity (1.48 V) which is impossible because heat is produced.

Gibbs free energy (ΔG_r) permits to convert chemical energy directly into electrical energy. Variations in Gibbs free energy of the reaction corresponds to the electric work done by the reaction (*n.F.E*).

$$\Delta G_r = -n.F.E \quad [2]$$

E corresponds to the theorical voltage. At standard pressure and temperature conditions, the theorical voltage available in fuel cells is egal to 1.23 Volts which is the maximal theorical voltage for a fuel cell (impossible to reach in reality).

Because the pressure and concentration of reactants affect the Gibbs free energy (thus voltage), it is necessary to use equation taking account of these parameters. The Nernst equation takes account about pressure and concentration b and is expressed like:

$$E = E^0 - \frac{R.T}{n.F}.\ln\left(\frac{\prod Y_{Products}^{v_i}}{\prod Y_{Reactants}^{v_i}}\right) \quad [3]$$

Where E^0 is the voltage at standard pressure and temperature conditions (i.e. 1.23 Volts), *R* the perfect gas constant (8.314 $J.mol^{-1}.K^{-1}$), T the absolute temperature in Kelvin, *Y* is the activity of the products and v_i the stoichiometric coefficients of species *i*.

In addition of equations to determine the voltage of fuel cells, it is interesting to take an interest in the different losses. In total, there are three different types of losses that govern fuel cells: activation losses, ohmic losses and mass transfer losses.

Activation losses is a phenomenon which occur mainly in the low current densities. This can be explained because in the low current density region, the working potential decreases, mainly due to the charge transfer kinetics, (i.e. the rates of O_2 reduction and H_2 oxidation at the electrode surface). Activations losses can be expressed by the Tafel equation which is written as follows:

$$\Delta V_{act} = a + b.\log(j) = -\frac{2.303.R.T}{\alpha.n.F}.\log(j_0) + \frac{2.303.R.T}{\alpha.n.F}.\log(j) \quad [4]$$

With j_0 the exchange current density (electrode activity for a particular reaction at equilibrium) [$A.cm^{-2}$].

Ohmic losses occur in the intermediate current density range and are mainly caused by internal resistance. Internal resistance (*Rcell*) corresponds to the flow of electrons through material and electrodes, interconnections but also resistance to the ionic flow through the electrolyte. Ohmic losses can be written as:

$$\Delta Ohm = j.Rcell \quad [5]$$

Mass transport losses (also named concentration losses) operate mainly in high current density range. It corresponds to the losses due to the transfer speed of reactants which is slower than reaction rate. Mass transport losses can be expressed as:

$$\Delta conc = \frac{R.T}{n.F}.\ln\left(\frac{C_R^0}{C_R^*}\right) \quad [6]$$

Where C_R^0 is the bulk concentration of reactant and C_R^* is the reactant concentration on the catalyst layer. Accumulation of product is ignored in this equation.

- Polarization curve (I-V)

Polarization curve is the most popular electrochemical technique to evaluate fuel cells performances. It consists in a plot which show the cell (or system) voltage change with current density. I-V curves provide information about the voltage and are also used as indicators of overall performance under specific operating conditions. However, they do not give much information about the individual components within the cells. All performances losses can be view on I-V curve.

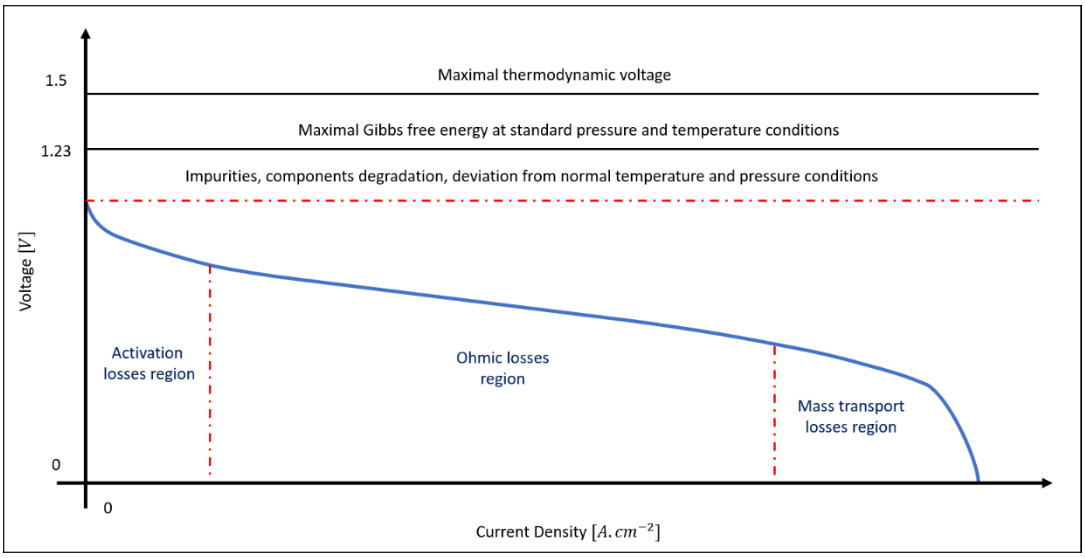

Figure 6 : Schematic representation of an example of polarization curve

Polarization curves are effective techniques for obtaining accurate information on the general health of the fuel cell, moreover, they do not need specific equipment compare to others diagnostic tools. However, this technique cannot be used when the system is operating. In fact, I-V curves require the measurement of the system voltage at different current densities and therefore to wait for each measurement point to stabilize the voltage.

In (Mohsin et al., 2020), PEMFC assemblies studied by an accelerated voltage cycle at several levels of relative humidity were characterized with polarization curves.

- Cyclic Voltammetry

In situ cyclic voltammetry is an electrochemical technique regularly used because it offers a multitude of experimental information and knowledge about the kinetic and thermodynamic details of many chemical systems. It measures the current response of an active redox solution to a linear-cycle potential (applied by a potentiostat) scans between two (or more) values. In situ cyclic measurement of voltammetry of fuel cells is carried out using a two electrodes device (working and counter electrodes), where the potential relative to a reference electrode is scanned at a working electrode while the resulting current flowing through a counter-electrode is monitored. Figure 7 shows a typical plot of a cyclic voltammogram:

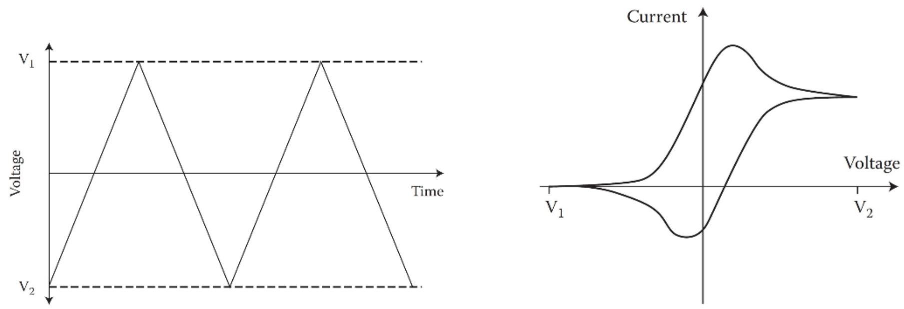

Figure 7 : Typical plot of a voltage sweep nack and forth between two voltage limits (left) and a cyclic voltammogram(right) (Wang et al., 2012)

The electrochemical activity of the fuel cell cathode is generally the most interesting information due to the slow kinetics of the Oxygen Reduction Reaction (ORR). The fuel cell anode is used as a counter or reference electrode, with the inherent assumption that the polarization of this electrode is relatively low. Cyclic voltammetry is a powerful electrochemical tool used to determine the Electrochemical Active Surface Area (ESCA) change in an electrode. However, cyclic voltammetry gives mainly qualitative and not quantitative information. It is therefore impossible to study the reaction and degradation mechanisms in depth.

In (Wang et al., 2014), the influence of PEMFC system contaminants on Pt Catalyst is evaluated via Cyclic Voltammetry.

- Linear Sweep Voltammetry (LSV)

Linear Sweep Voltammetry is an electrochemical method frequently used to estimate the gas crossover through membranes in PEMFC. It can be applied directly under different operating conditions. Full or supersaturated humidification conditions are generally used for fuel and inert gas to ensure that sufficient water is present for complete hydration of the membrane. LSV technique consists of applying a linear potential scan (thanks to a potentiostat) on the electrode to obtain a limit current. This limit current permits the calculation of the cross-over rate of hydrogen to cathode side. The use of linear sweep voltammetry is similar to cyclic voltammetry because it uses a counter-reference electrode (generally anode) and a working electrode (generally cathode). As with cyclic voltammetry measurements, in LSV measurements, the current response is plotted as a function of voltage rather than time. Figure 8 shows a schematic of the principle of LSV measurements and a typical LSV curve:

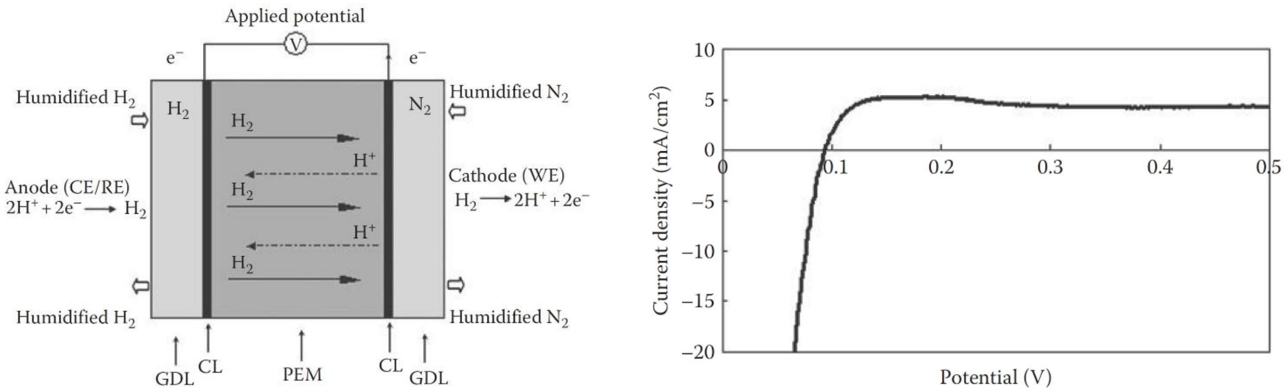

Figure 8 : Schema of the principle of LSV measurement in PEMFC (left) and typical LSV curve measured at 60 °C for a commercial Nafion membrane under 100% humidification (Wang et al., 2012)

Hydrogen cross-over flux J_{xover} [mol.cm^{-2}.s^{-1}] is determined by Faraday's law:

$$J_{xover} = \frac{j_{lim}}{n.F} \text{ [7]}$$

Where j_{lim} is the transport limiting current density [A.cm^{-2}], n the number of electrons which take part in the reaction (2 for H_2 oxidation reaction) and F the Faraday's constant (96 485 C.mol^{-1})

LSV is a powerful analytical tool to characterize fuel cross-over through PEMFC membranes. It can give quantitative results for the membrane that cover the entire active surface without damaging the membrane. In addition, LSV technique allows the detection of short-circuit resistance.

In general, LSV is an excellent diagnostic method for membrane evaluation and failure diagnosis in PEM fuel cells. Although it only reflects the crossing of gases at a medium level accuracy and sensitivity for membrane diagnosis are excellent. LSV is also useful for analysing mechanisms and predicting degradation, providing information prior to post-mortem analysis.

In (Pei et al., 2018), an improved LSV methods to measured hydrogen cross-over current in PEMFC is developed.

- Current Interruption (CI)

The current interruption consists in supplying a constant current to the electrochemical system and then passing instantaneously at zero current, while recording the change in system or cell potential. Generally, the current is interrupted from microseconds to second level. Current interruption permits to measure the value of the membrane resistance because once the current interrupted, ohmic losses disappear almost immediately and activation losses overpotentials decline to Open Circuit Voltage (OCV) slowly. So, a rapid acquisition of voltage evolution is mandatory to separate ohmic and activation losses.
Relationship between the membrane resistance and voltage step height is given by:

$$R_{mem} = \frac{\Delta U}{\Delta I} \text{ [8]}$$

With ΔU is the voltage variation [V], ΔI the current drop [A.cm^{-2}] and R_{mem} the membrane resistance *[Ohm.cm^{-2}]*

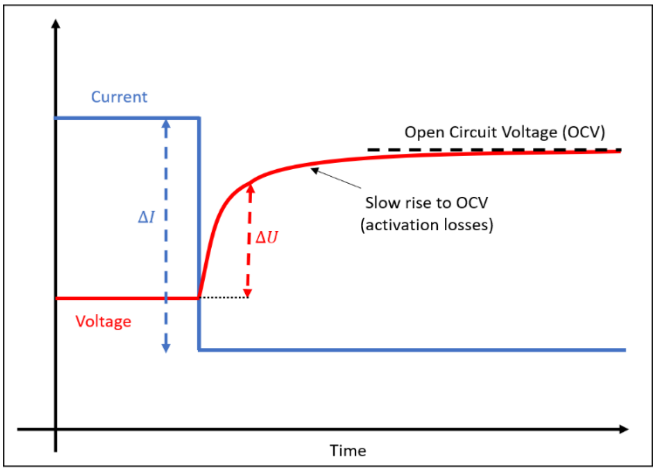

Figure 9 : Schematic representation of current interruption

Current interruption is a useful tool for characterizing the dynamic behaviour of electrochemical devices. Compared to other methods, power interruption has the advantage of being simple for data analysis. Nevertheless, the information obtained is limited to the membrane resistance and, moreover, it is difficult to determine the exact point where the voltage jumps. A fast oscilloscope is therefore required to record the voltage jump.

In (Mennola et al., 2002), current interruption method is used to measure the ohmic voltage loss in a single cell PEMFC.

- Electrochemical Impedance Spectroscopy (EIS)

Impedance analysis is a popular and non-destructive measurement technique that provides detailed information on a wide range of electrochemical phenomena such as the charge transfer reaction for example. The EIS technique involves applying a low-level alternating current waveform to the fuel cell system (or any electrochemical system) and then measure the response of the system (or cell) to the stimulus. The impedance is measured using the ratio of AC voltage divided by AC current:

$$|\bar{Z}| = \frac{AC\ voltage}{AC\ current} \quad [9]$$

Figure 10 represents an EIS applied to a fuel cell system.

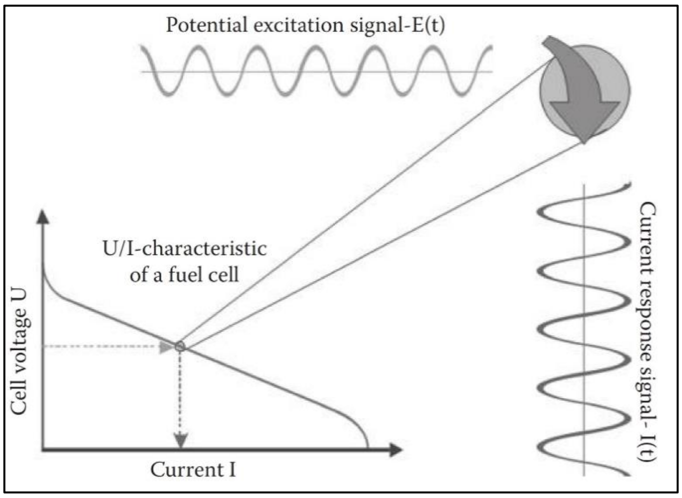

Figure 10 : Schematic representation of EIS applied to fuel cell characterization (Wang et al., 2012)

Because the AC stimulus application has a low amplitude, there is no perturbation or destruction of the monitored cell. Generally, frequencies used for EIS are in the range [0.1, 100.10^3] Hz, AC waveform is generated by a potentiostat which provides signal conditioning, amplification and DC/AC control to correctly apply the stimulus. In addition, the potentiostat provides a current-to-voltage conversion circuit to convert the alternating current flowing through the cell into an alternating voltage waveform that can be measured by a frequency response analyzer (FRA) to provide impedance analysis. The measured impedance can be represented in Nyquist and Bode diagrams. In the section 3 , EIS measured are analyzed in Nyquist and Bode diagrams. EIS are very useful tools which can measure detailed parameters such as the polarization resistance used to determine the corrosion current density. The main advantage of this method is that it allows the capture of information that appears with different time constants (thus different frequencies), which is not possible with I-V curves. For example, mass transports phenomena occur at low frequency range while charge transfers at high frequency range. Nevertheless, EIS requires specific equipment that can be expensive and difficult to implement in fuel cell systems.

In (Mérida et al., 2006), EIS has been used to distinguish between flood and dehydration failure modes.

In this paper, the selected diagnosis tool is the electrochemical impedance spectroscopy. Interest in this choice is that EIS gives a lot of specific information for main fuel cells faults because it analyzes the dynamic response of several phenomena. Furthermore, a dedicated power converter at the output of the fuel cell has been developed in the HealthCode project to allow the online measurement in real life application. Voltammetry method (CV and LSV) are not suitable for the diagnosis of operating fuel cells because they need to introduce hydrogen and nitrogen through the anode and cathode of the cell, i.e. changing the feeding gas and interrupting the power supply to the application. Polarization curves can be used for on-board diagnosis however it contains less information than EIS even if it is an easier process.

2 Designed diagnosis approach

The method presented below uses a fuzzy C-means classifier to classify data recorded during EIS. Firstly, a global presentation of the method is made, then an explanation about the off-line and on-line section is proposed followed by the presentation of results obtained.

2.1 General principle

According to the explanations given in section 1, the developed algorithm is composed of several steps: An extraction of features from the data collected from the EIS, a standardization using Quantile Transformer of the features followed by a selection of the ones containing the most information using the Pearson Correlation Coefficient (PCC) and the F-Test ANOVA. The last step of this algorithm is the classification of data using the Fuzzy C-Means clustering. The principle of the designed algorithm is presented in Figure 11:

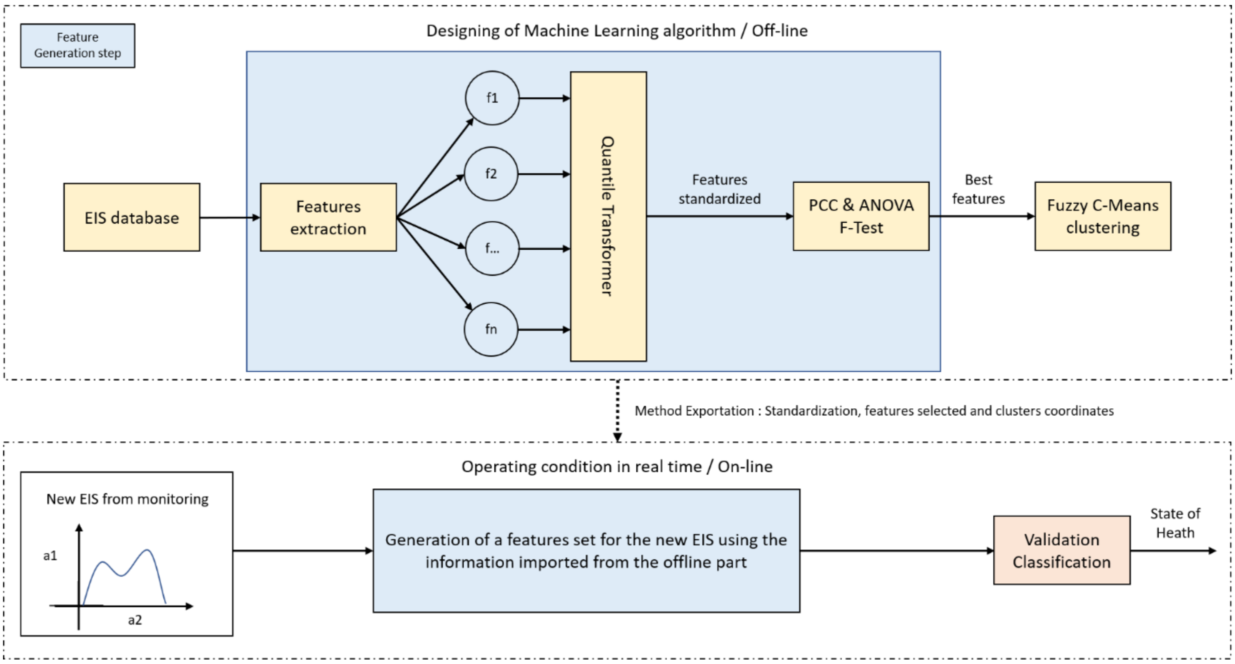

Figure 11 : Schema of the developed classification algorithm

As the Figure 11 shows, the steps of features extraction, standardization and features selection are grouped in one global step named "Feature generation".

2.2 Off-line / Training

As explained, off-line section of non model-based algorithms are composed of two steps: Generation of features and Classification. In the case of the designed algorithm, the data used are from electro-chemical impedance spectroscopy monitoring. Impedance information given by EIS is decomposed in a real and imaginary parts or magnitude and phase which are used to create several features. In the developed diagnosis, the first extracted features from EIS are:

- the Minimal magnitude (*mm*) of the impedance which indicates the total Ohmic resistance of the stack, (1)
- the Maximal magnitude (*Mm*) of the impedance (2), which is included to analyze stack incomplete spectra where polarization resistance is not given.
- the difference between both magnitude (*ΔMag*), (3) which corresponds to the width of spectrum and gives information about the mass transport rate of reactants.
- the polarization resistance (*R_pola*), which gives information about global performance of FC stack (4)
- the maximal phase (*Mp*), which provides information on electrolyte membrane-related degradations (5)
- the minimal phase (*mp),* which provides information about the charge transfer of Hydrogen oxidation reaction (6)
- the phase at a frequency of 0.1 Hz (*P1*) to observe phenomena of diffusion. (7)
- the difference between P1 and Mp (*ΔPha)* which permits to observe the height of *phase spectrum.* (8)
- also, an analysis of phase is done using the Bode diagrams. The objective of this analysis is to describe the phase as a first order equation of frequency (*f*) in the low frequency range [1 – 10] Hz.

$$Phase = A.f + B1 \text{ [10]}$$

Coefficients A (*Coeff A)* and B (*Coeff B*) are determined for each sample and are used as features (9 & 10). They allow obtaining information on charge transfer of oxygen reduction reaction.

Figure 12 shows an example of Nyquist and Bode diagram for a fuel cell.

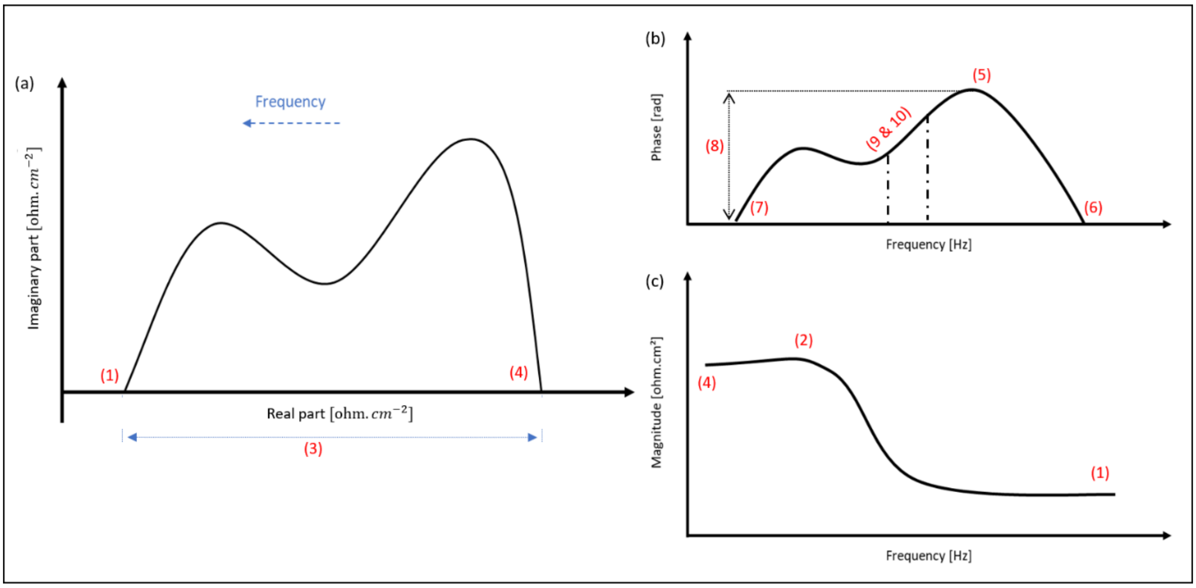

Figure 12 : Example of Nyquist (a) and Bode (b, c) plot for an EIS

Feature extraction allowed switching from a two-dimensional space (Real and Imaginary parts) to a multi-dimensional space (10 features before the selection phase).

Once the first dimensional space is created, each feature is standardized so that it follows a uniform distribution law. The "Quantile Transformer" standardization method used requires a certain number of quantile (number of reference points used to discretize the cumulative distribution function) to be filled in. Within the framework of the studied algorithm, the number of available samples being small (less than 100) the number of quantiles to be used is equal to the number of samples. As a reminder, this standardization method has been selected because of its high capacity to handle outliers and noisy data which are generally present in experimental test of fuel cells.

The last step to generate the best features to optimize the classification process is selection. As previously described, in this paper the selection is based on a data filtering step using the Pearson correlation coefficient followed by an ANOVA F-Test. For this study, the absolute value of the PCC that has been retained is 0.9, which means that features that have 90% correlation (positive or negative) are not directly selected. The variance of each feature is compared and only the feature with the highest variance is kept. Then the ANOVA F-Test is used to sort the features by analyzing the relationship of each feature with the associated fault. The optimal number of features for each technology has been determined through an iteration process. Section 4.2 shows the evolution of the classification results according to the number of features selected.

Once best features selected, the classification step can occur. Fuzzy C-means clustering creates clusters (and determines coordinates of each cluster center) for each fault used in database. C-Means clustering is an unsupervised method in the sense that the centers and the labels of the clusters are not determined a priori. However, the expertise of the user is involved in the design of the database on which the learning is carried out, so available information is used to optimize the creation of clusters. Then, the user can provide the number of faults and the number of levels for each fault. For example, for the creation of clusters associated with three dryness levels, the user will only fill in the dryness data and the number of faults levels. In our case, we will define 3 levels for low, medium and high dryness. This allows an unsupervised operation which requires some knowledge of the database. Fuzzy C-means clustering is the chosen method because of its low computing time and good accuracy. However, the biggest drawback of this method is that it may lack robustness. This is due to its initialization when the algorithm associates each point to a cluster. Therefore, it is important to properly generate the features. In the following sections, the development of the training algorithm applied to the PEMFC diagnosis using EIS is presented. Figure 13 shows the off-line section of this algorithm diagnosis.

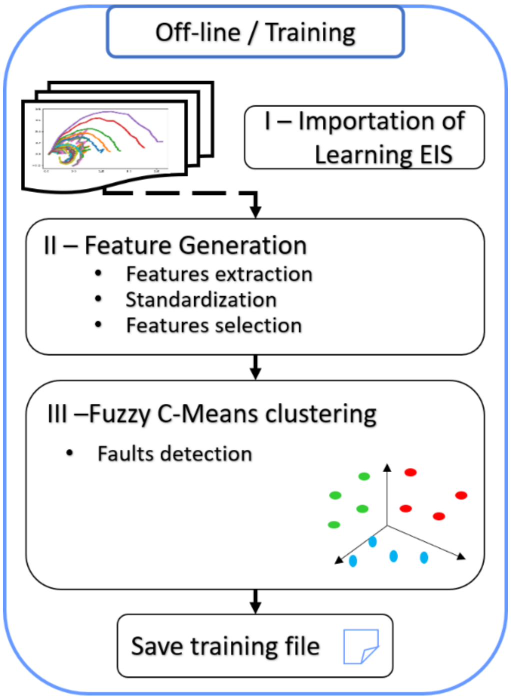

Figure 13 : Principle of the off-line part of the designed diagnosis

2.2.1 Specific case: Carbon Monoxide Detection

Even if the principle of the algorithm is identical for the two stacks tested, it can be modified in order to adapt to the tested defects. In the case of the H2/Air technology the carbon monoxide (CO) poisoning defect of the cathode is

tested. This part is more detailed in section 3, however it is interesting to know that it is possible to detect high CO poisoning from a single feature which is the imaginary part at low frequency.
To isolate this specific fault, a new step is added in the algorithm before the generation of features. This step doesn't need any standardization or feature selection because of the specification of the fault. To detect it, the new classification step uses a FCM clustering algorithm to build two clusters using the imaginary part of EIS data at low frequency (i.e. 0.1 Hz): the first cluster is created using the EIS data with a high level of CO poisoning and the second one using all the other data.

2.3 On-line / Validation

The on-line algorithm is implemented onboard to perform the diagnosis all along the lifetime of the system. It consists the acquisition of a new EI Spectrum and the diagnosis algorithm is run in order to determine to which cluster determined in the training step it belongs. On-line is linked to off-line because even if it is in real time, it uses information imported from off-line. In the case of the developed diagnosis, information imported from off-line are: information contained in the standardization to transform the new characteristics to the same scale, the best characteristics selected, the coordinates of the clusters determined by the FCM grouping and their membership (i.e. the fault) assimilated to each cluster. To assign a defect to the new EIS, the algorithm will calculate the Euclidean distance between this point and all imported clusters. The fault associated with the closest cluster will also be the one assigned to the new EIS.
In the specific case of carbon monoxide poisoning cluster coordinates of the two clusters (one for high CO poisoning and one for all other faults) are also imported.

Figure 14 and Figure 15 show how the on-line part of diagnosis is done.

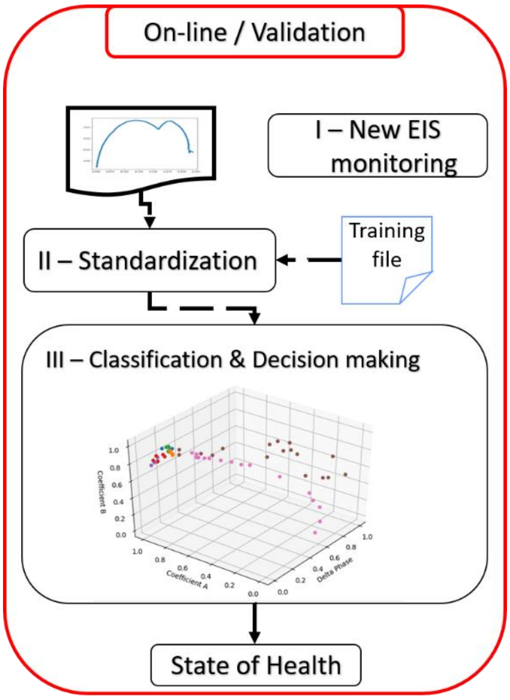

Figure 14: Principle of on-line part of the designed diagnosis

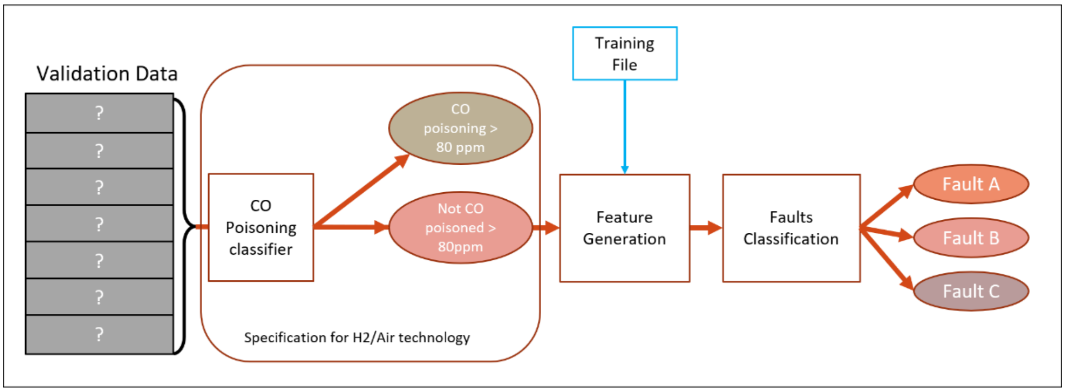

Figure 15: Presentation of diagnosis algorithm

In order to validate a diagnostic algorithm before implementing it in a system to test it experimentally, it is interesting to test the algorithm with data from the database.

To proceed to this validation, it is possible to divide its database in two parts with for example 80% of data used for training (off-line) and 20% of data that will be used to validate it (simulation of an on-line part). This method of validating the algorithm is not optimal as the results can vary depending on the distribution of the data. It does not give a global idea of the performance of the diagnosis. In order to remedy this concern and to have a global idea of the performances, cross-validation is used. The following section is dedicated to the presentation of the cross-validation method used.

2.4 Cross-Validation

Cross-validation is a statistical method for evaluating the generalization performance of a diagnostic algorithm. This statistical method consists in dividing the database into several parts (k parts) in order to train it with k-1 parts and test it on the last part. There are different methods of cross-validation such as "K-Fold" cross validation but the method that has been retained here is the "Leave One Out" (LOO).

LOO method is an iterative process which consists of using all data for the training except one which is used for the validation. Thus, for n samples, there are *n* different training and *n* different test sets. For each loop, both accuracy results are extracted (i.e well classification of learning and validation dataset). At the end of LOO cross-validation, the mean of accuracy results for learning and validation is computed. This permits to have global results useful to characterize the generalization of the diagnosis. In reference (Shaikh, 2018) a presentation of several methodologies for cross validation is done. Figure 16 explains the principle of LOO methodology with a dataset composed of 5 data:

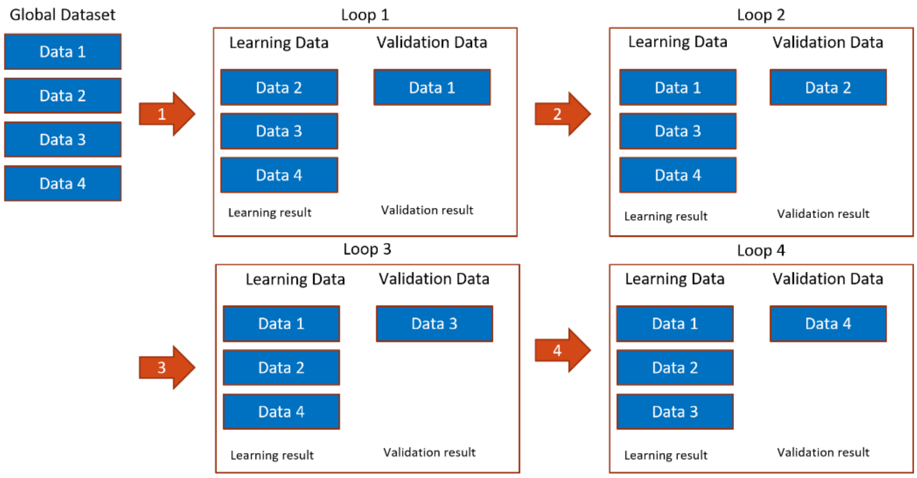

Figure 16: Presentation of the Leave One Out methodology

2.5 Performance Index

In order to be able to analyze the results obtained during cross-validation, it is important to define performance indices. These indexes correspond to all the parameters that will be analyzed in order to understand the functioning of the algorithm as well as possible. For this study three indices were defined: The confusion matrix, the precision score and the analysis of the features selected by the algorithm.

These three indices allow having a global idea of the performances (accuracy score), to understand at best the errors that the algorithm can make when it assigns a fault to a data but also to make a link with the physics of the phenomena composing a fuel cell (analysis of feature selected). Indexes will be developed in the following section.

- Confusion Matrix

To analyze the results, metrics are considered to assess the performance of the diagnostic approach. For this purpose, the confusion matrix (also named as contingency matrix) is selected. The confusion matrix is very useful in diagnosis because for a specific condition “f” it permits to view the 4 specific cases which are:

- “a” the number of samples correctly assigned to “f”
- “b” the number of samples mistakenly assigned to “f”
- “c” the number of samples mistakenly not assigned as “f”
- “d” the number of samples correctly not assigned as “f”

Figure 17 displays an example of confusion matrix:

	Confusion Matrix	
	True condition ?	
Diagnosed condition ?	Yes	No
Yes	a	b
No	c	d

Figure 17: Example of Confusion Matrix

Several indicators to evaluate a fault diagnosis performances are proposed(Cadet et al., 2014).

- Accuracy score

Besides the uses of confusion matrix, the accuracy score is selected to evaluate the diagnosis approach. It represents the percentage of good classification that the algorithm has achieved. Accuracy score can be defined using metrics presented in confusion matrix:

$$Accuracy = \frac{number\ of\ correctly\ classified\ data}{total\ number\ of\ data\ classified} = \frac{a+d}{\mathrm{a+b+c+d}} \quad [11]$$

- Analysis of features selected during cross-validation

Because the developed feature selection is based on an automatic process, it is possible to observe some modifications of features selected during the cross-validation. It is however interesting to look at the number of times each feature has been selected because it permits to determine which ones represent the best a database. In case of the whole database is sufficient, and there is not high difference of scaling between features, the same features should be selected at each loop of the LOO. However, if the same features are not selected, it may significate that the database is not sufficient and/or that a single data may impact the selection of the best features due to it difference of scaling with other data.

3 Experimental tests and acquired database

The Electrochemical Impedance Spectroscopy (EIS) is a widely used technique at the laboratory scale to investigate the operation of electrochemical devices. The Health-Code project ("Real operation pem fuel cells HEALTH-state monitoring and diagnosis based on dc-dc COnverter embeddeD Eis," n.d.) has demonstrated that the technique can be embedded through the use of the power converter of the fuel cell in real-life application and carried out on-line. The spectra measured that way can then be used for on-line diagnosis input.

The data presented in this article and used for the training and the validation of the diagnosis algorithm have been acquired with laboratory devices on testbenches. The objective of experimental tests achieved is to characterize two different types of stack under several faulty conditions. The first is an H_2 - O_2 stack and the second is an H_2 - Air.

The diagnosed faulty conditions tested in this paper are the improper water management (drying and flooding), the reactants' starvation (fuel and oxidant) and the altered fuel quality by contaminations (CO and S Poisoning).

3.1 Presentation of faults tested

According to (Wang, n.d.), during oxidation and reduction of reactants in a fuel cell, electrochemical reaction can occur in front or in the electrode. Moreover, mass transport hindrance and concentration gradient can impact FC performances. These different reactions occur with different time constants ranging from microseconds to months.

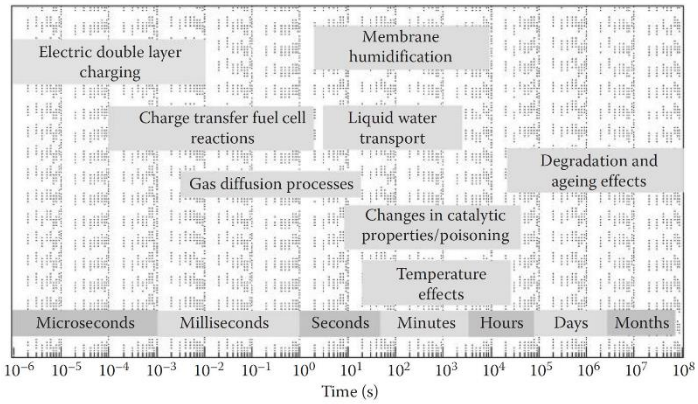

Figure 19 : Overview of the wide range of dynamic processes in fuel cells (Wang, n.d.).

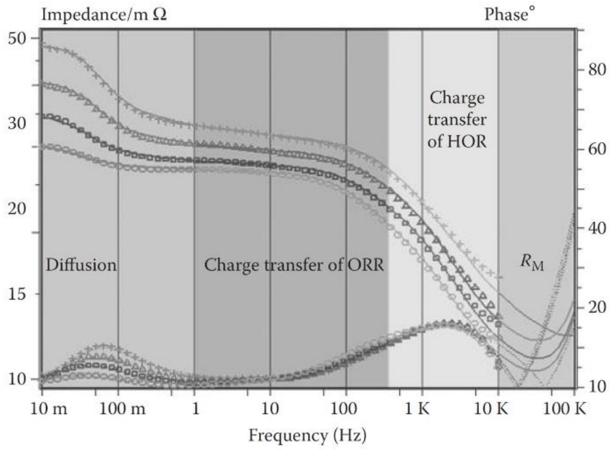

Figure 18 : Bode plot of EIS measured at different current densities, PEMFC operated at 80°C with H2 and O2 at 2 bars (Wang, n.d.).

Figure 18 shows these different time constants which are described in (Wagner and Friedrich, 2009) and Figure 19 shows the impact of these time constants in the frequency domain.

In the next of this section, a presentation of fault tested and their mechanisms is done.

3.1.1 Water management (Flooding & Drying)

According to (Yousfi-Steiner et al., 2008), PEMFC performance, life-time and stability are highly linked to water management. Globally, two water flows can be observed in a fuel cell: the electro-osmotic drag and the back-diffusion. Electro-osmotic drag corresponds to the water brought by proton transfer between anode and cathode side because of the apply potential across the membrane, while back-diffusion depends on water gradient between both sides. If the flow of water (from supplying/electroosmosis/back-diffusion) are not properly managed, two phenomena can occur: flooding and drying, which depends on whether the water balance is in excess or in defect.

Drying results from the combination of high temperature, low current and poor water management. It is more likely to occur at the anode side of the membrane due to the production of water at cathode side. This leads to dehydration of the membrane and a decrease in proton conductivity through the electrolyte (sulfonic acid bond cannot be dissociated and the protons cannot jump between acid group) (Hickner et al., 2006). In addition, drying causes a decrease in reaction sites (catalyst + protons + electrons + reactive gases) which leads to an increase in activation losses. Brief exposure to this phenomenon leads to losses that can be recovered. However, at high drying intensity, hot spots may appear that can pierce the membrane and create pinholes. Also, long-term drying may promote further chemical reactions at reactive sites that can no longer be properly moistened (Schmittinger and Vahidi, 2008).

In contrast to too little water management, too much humidity in the reactive gases of a fuel cell can also lead to flooding. High reactants' relative humidity (RH) combined with low gas flow rate and low temperature are the main causes of flooding. Accumulation of water in the gas diffusion layer (GDL) can prevent proper distribution of reactants to the reaction sites. Flooding takes place in two stages: first, drops of water will cause a slow decrease in voltage, and then the water accumulated in the channels causes blockage of the reactants and leads to a rapid degradation of the voltage (Fouquet et al., 2006). As for drying, short exposure to flooding conditions induces reversible losses but in case of long-duration, carbon corrosion and platinum dissolution phenomena occur (Schmittinger and Vahidi, 2008).

3.1.2 Reactants starvation phenomena

There are two types of reactant starvation in a fuel cell: the starvation at the cathode which can be either a lack of pure oxygen or a lack of air and the starvation at the anode which corresponds to a lack of hydrogen. Starvation can occur in one or several cells depending on fuel supply. Fuel starvations are more harmful than oxidant starvations (Yousfi-Steiner et al., 2009, 2008). Starvation can be broken down into two categories: local and global starvation.

Local starvation results from a non-homogeneous distribution of gases at the reactive sites along the catalytic layer. This heterogeneous gas distribution results in heterogeneous current distribution due to the limitations imposed by local mass transfer. This may be caused by a too low reactant flow rate to consume all reactant to the maximum.

Global starvation occurs when the reactant is not sufficient for electrochemical reactions to occur. This usually occurs when the fuel cell starts up or when there is a sudden surge in current. The limitations of mass transfer will gradually decrease the voltage. In the case of a starvation at anode side, hydrogen oxidation reaction will not be able to deliver the amount of current driven by cells which function in nominal conditions. Therefore, since fuel cell stacks operate in galvanostatic mode and since the cells are all connected in series, a starving cell can be forced to operate in reversal mode in order to maintain current flow at the value fixed by cells located upstream from it. These cells will make the starving cell operate in an electrolysis mode by providing the needed energy. Consequently, the individual voltage of starving cells become negative and their anode potential increases until reaching a value at which other oxidation reactions could occur in order to maintain the charge flow. Depending on the value reached by the potential, these reactions can be platinum dissolution reaction, carbon corrosion and, in case of cell reversal, water electrolysis. Such cell reversal is a rapid source of irreversible degradations.

3.1.3 Fuel Poisoning (Carbon Monoxide & Sulfur)

The main catalyst used for PEMFC is platinum or platinum alloys. This choice can be explained because platinum has excellent properties to facilitate oxygen reduction and hydrogen oxidation. However, platinum is also a good catalyst with other chemical species such as sulfur compounds (SO_2, H_2S, sulfites), nitrogen compounds (NO_2, NO, NH_3) and carbon monoxide (Zhao et al., 2020). These contaminants come from activities related to motor vehicles, industry, and gas treatment. Depending on the contaminants present in the reactive gases, two types of degradation may occur: a reduction of the platinum oxide due to the removal of CO formed during carbon corrosion or a dissolution/redeposition of the platinum bound to the agglomeration and detachment/corrosion of the carbon (Zhang et al., 2009). Reduction of platinum is a recoverable loss while dissolution/re-deposition is uncoverable.

Currently, natural gas reforming is the most common production method, according to IEA "less than 0.1% of global dedicated hydrogen production today comes from water electrolysis" ("The Future of Hydrogen – Analysis," n.d.), however, this process produces carbon monoxide (CO) and carbon dioxide (CO2). The effect of CO is mainly due to its high adsorption affinity to platinum. The CO is adsorbed on the reaction sites and replaces the hydrogen already present. Once on the reaction site, the CO will prevent the adsorption of hydrogen which will reduce the active surface dedicated to the electrochemical reactions. As a result, the local current density increases, which in turn increases the anodic activation overvoltage. High CO concentrations increase this potential high enough that the electrochemical potential of the anode reaches the value at which the CO oxidizes into CO_2, thus releasing the reaction sites and decreasing the anodic potential to its initial level. Because of this adsorption/release phenomenon of the reaction sites, the cell/stack voltage oscillates during operation due to the oscillation of the active surface. However, even if this phenomenon is reversible, kinetic adsorption is faster than desorption. To accelerate that (Farrell et al., 2007) presents three methods :

- Air bleeding which consists to add a low concentration of air in the fuel. It permits to remove faster CO but can cause overheating at the anode if air management is improper.

- Use of CO tolerant catalyst such as Pt/Ru, but even if this combination results in a reduction of cell potential compare to pure platinum, this solution is less efficient that the use of pure hydrogen as fuel.

- Periodic pulsing of the anode potential. The principle of this method consists in briefly applying an impulse to reach an anodic potential level high enough to oxidize CO into CO_2.

In addition to CO poisoning, which is responsible of platinum reduction, sulphur poisoning is responsible of irreversible loss of reaction site. Sulphur can be present in fuel in different forms depending on the source of hydrogen and air quality. When hydrogen comes from the reforming of hydrocarbons, it is possible to find up to 5ppm H2S after desulphurization (Sethuraman and Weidner, 2010; Zhao et al., 2020). But in addition to the sulphur present during the reforming of natural gas, it is possible to find traces in the ambient air that can enter the cathode of a PEMFC.

Poisoning kinetics of H_2S on composite solid polymer electrolyte (SPE-Pt) electrode takes place by dissociative adsorption on the SPE-Pt electrode as two forms of sulphur species, and under favourable potential it undergoes electro-oxidation to sulphur and then to SO_2 (Sethuraman and Weidner, 2010). So, the adsorption potential is what dictates the sulphur coverage and authors suggest that the overpotential of PEMFC exposed to H_2S should be kept below the equilibrium potential for sulphur oxidation to minimize irreversible loss of catalyst site. According to (Lopes et al., 2011) the poisoning extent and mechanisms depend on factors like potential, temperature and Pt loading.

Unlike carbon monoxide poisoning, sulphur causes irreversible damage. This means that if the fuel supply is not purified and the stack is shut down, other reactions may occur such as carbon corrosion. Therefore, high potential and high current density operating conditions should be avoided to minimize irreversible sulphur poisoning.

Although it is impossible to fully recover losses due to H_2S, techniques to partially recover reaction sites have been proposed:

- Combination of neat hydrogen and cyclic voltammetry scan could recover partially performance of fuel cells poisoned (Shi et al., 2007)

- Temperature and the platinum load would also favour a partial recovery after sulphur poisoning (Sethuraman and Weidner, 2010).

- The use of a graphene supported platinum electrode which has a slower degradation and faster recovery compared to Vulcan carbon supported platinum electrodes (Jayaraj et al., 2014).

3.1.4 Influence of cathodic gas

Since the two stacks tested do not use the same cathode reactant (one pure oxygen and the other ambient air), it is interesting to compare the impact of the gas type on a stack. In (Wang, n.d.) a comparison between a O2 fed and an Air fed stack is done. It shows that when operating with air, two sources of performance losses can be found at the cathode:

- The first is an increase of the charge transfer resistance due the decreasing of oxygen partial pressure.
- The second is an additional diffusion impedance term which appears in the low frequency domain.

Figure 20 is from (Wang, n.d.) and shows the both sources of performances losses. Diffusion impedance term is visible at 3 Hz.

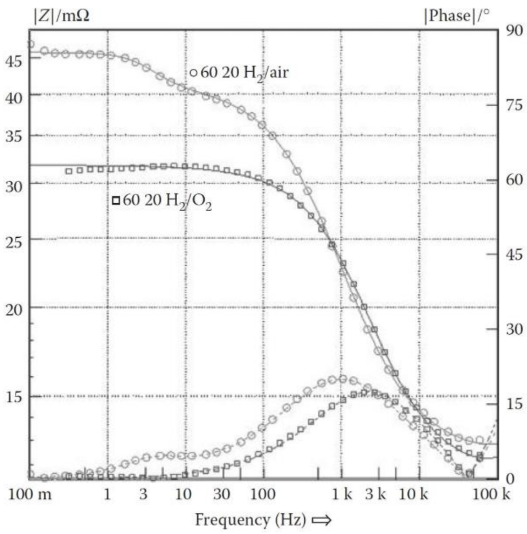

Figure 20 : Comparison of EIS measurements (Bode plot) of the same MEA (60 20) produced with carbon supported (60 wt% Pt) catalyst and 20 wt% Nafion, operated with H2/O2 (□) and with H2/air (○) at 500 mA cm−2 (Wang, n.d.).

3.2 Presentation of fuel cells

3.2.1 H2/O2 short stack

The experiments are carried out on a short stack to limit the cost of the testing campaign. As it is supposed to operate with electrolyzed hydrogen in the targeted application, fuel contamination is not considered. More details on these tests can be found in (Petrone et al., 2018).

This short stack consists of 8 cells and a cell active area of 200 cm². The maximum power delivered by the short stack is about 1.3 kW while the complete system can deliver up to 3 KW. Tests are scheduled to reproduce the real back-up system operations that mainly operates between 0 and 240 A. For nominal test conditions, parameters are set to the values describes in the Table 2:

Table 2 : Nominal conditions used for H2/O2 short stack tests

Pressure Gas inlet anode	$1.36 * 10^5$	[Pa]
Pressure Gas inlet cathode	$1.42 * 10^5$	[Pa]
Anode Over-stoichiometry Factors (H_2)	1.9	[-]
Cathode Over-stoichiometry Factors (O_2)	2.9	[-]
Relative humidity (RH)	50% ± 10%	[-]
Stack temperature	335 ± 5 K	[K]

Based on the EIS methodology measurement, three DC currents have been retained for the short-stack tests:

- Maximal current at 210 A (nominal real operation condition)

- Minimal current at 45 A (# 20% of maximal electric load)
- Medium current at 120 A (# the mean of others)

3.2.2 H2/Air stack

H2/Air stack is a 1.3 kW stack with an active surface of 100cm². For nominal test conditions, parameters are set to the values described in the Table 3:

Table 3 : Nominal conditions used for H2/Air stack tests

Pressure Gas inlet anode	1.24 *10^5	[Pa]
Pressure Gas inlet cathode	1.15 *10^5	[Pa]
Anode Over-stoichiometry Factors (H_2)	1.3	[-]
Cathode Over-stoichiometry Factors (O_2)	2	[-]
Relative humidity (RH)	83.3%	[-]
Stack temperature	330	[K]

To cover real system operation, three DC currents have been defined for the EIS:

- Maximal current at 40 A (nominal real operation condition).
- Minimal current at 15 A.
- Medium current at 25 A.

3.3 Faults generation Protocols

This section explains how testing experiments were carried out.

Both stacks are run in a continuous mode, respecting suppliers' indications. They are periodically characterized via I-V curves (non-faulty conditions) and EIS (either in nominal or in faulty conditions).

3.3.1 General measurements

The first step of measurements is to plot the polarization curve (I-V curve) in a nominal condition. Then a current level is chosen and an EIS also in nominal condition is plot. Then a fault is introduced. 3 intensity levels are chosen for each tested fault.

Figure 21 shows a schematic representation of the general procedure of data collection about faults.

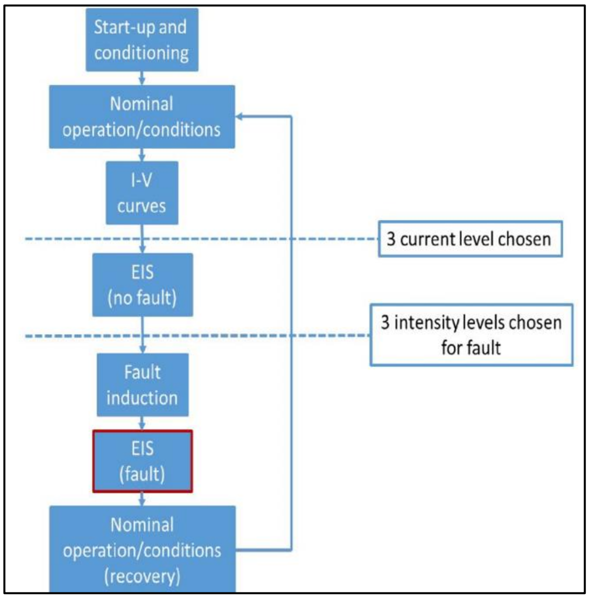

Figure 21 : From HEALTH CODE protocols, General representation of the measurement procedure ("Real operation pem fuel cells HEALTH-state monitoring and diagnosis based on dc-dc COnverter embeddeD Eis;H2020, European project, Horizon 2020; Health-Code," n.d.).

3.3.2 Protocol recommended for faults' creation

Concerning the faults, the recommended procedure consists of fixing the fault level and then changing the current density. Once the current density has reached the maximum value defined in the previous section, the system performances are recovered and carried out the same process with a higher fault level. The Figure 22 shows how the protocol is applied for starvation and water management:

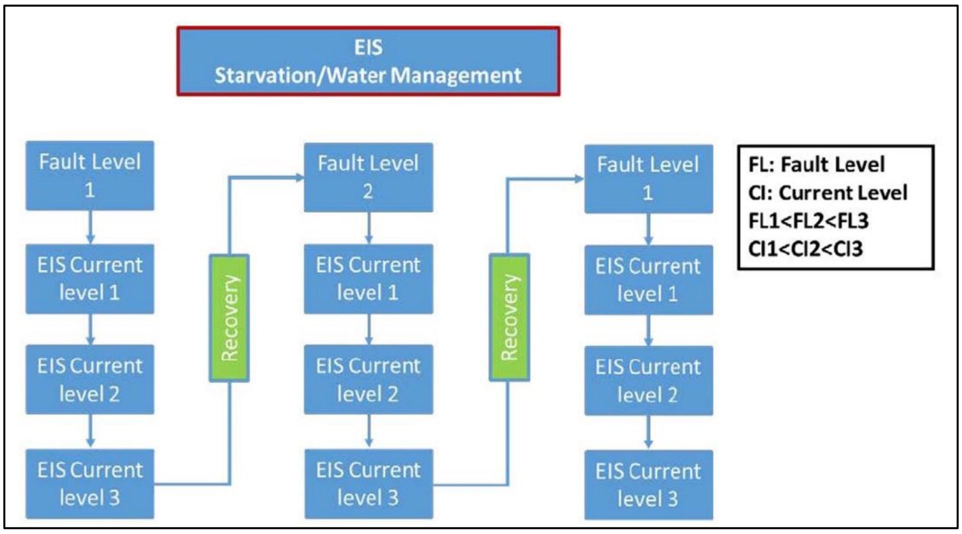

Figure 22 : From HEALTH CODE protocols, focus on the EIS measurement procedure recommended for Starvation and Water Management ("Real operation pem fuel cells HEALTH-state monitoring and diagnosis based on dc-dc COnverter embeddeD Eis;H2020, European project, Horizon 2020; Health-Code," n.d.)

The same process is recommended for Fuel Composition. This method permits to decrease the test duration because it accelerates the reaching of stack equilibrium.

I-V curves are measured in two phases. Firstly, a step-by-step current-increasing method is chosen and then the reverse process is done. The result is a polarization curve with an ascending and a descending section. EIS specifications

To control that protocol, fixed limits for the test are showed in Table 4:

Table 4 : Protocols, Variable inputs for EIS

Input	Value for laboratories test
Frequency	10 kHz – 10 mHz (log scale)
Current value	5-10% of DC or fixed values < 5 A
Number of periods	1 – 20 (depending on frequency)
Sampling frequency	At least 100 times the injected frequency

3.4 Presentation of datasets

A total of 2300 EIS spectra were acquired in total during the project, but for this study, a selection of the best EIS made at nominal current were retained for analysis. This represents a total of 164 EIS.

For the H2/O2 short-stack, relevant faults tested are flooding, drying and reactants starvation. Same faults are tested for H2/Air stack but because air is used, carbon and sulfur poisoning are added to operating conditions.

Figure 23 shows the decomposition of EIS:

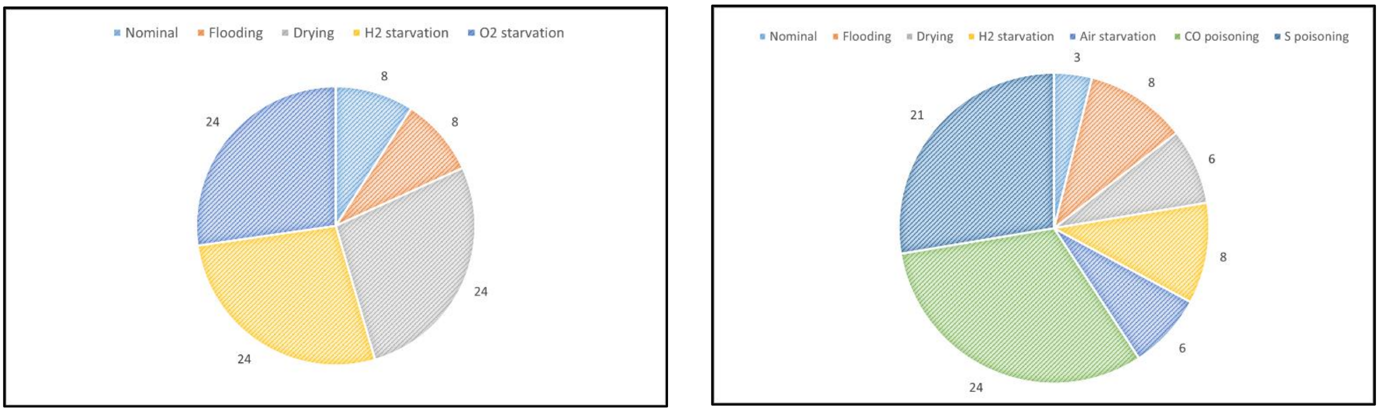

Figure 23 : Composition of dataset for H2/O2 stack for 1.05 A.cm-² (left) and for H2/Air dataset for 0.4 A.cm-² (right)

3.4.1 Presentation of EIS made for H2/02 short stack

Experimental tests using H2/O2 short stack were done at 3 current levels but to limit the number of graphics in this paper, only EIS done at 210 Amps are presented in this section. In each graph, an EIS in nominal condition is present to observe the magnitude impact of the fault.

Figure 24 compares three types of tests in the stack. The first one is in nominal mode, the second one is in flooding condition with only one level of degradation tested, the third one is in dry mode in which 3 different levels are tested (low, moderate and high).

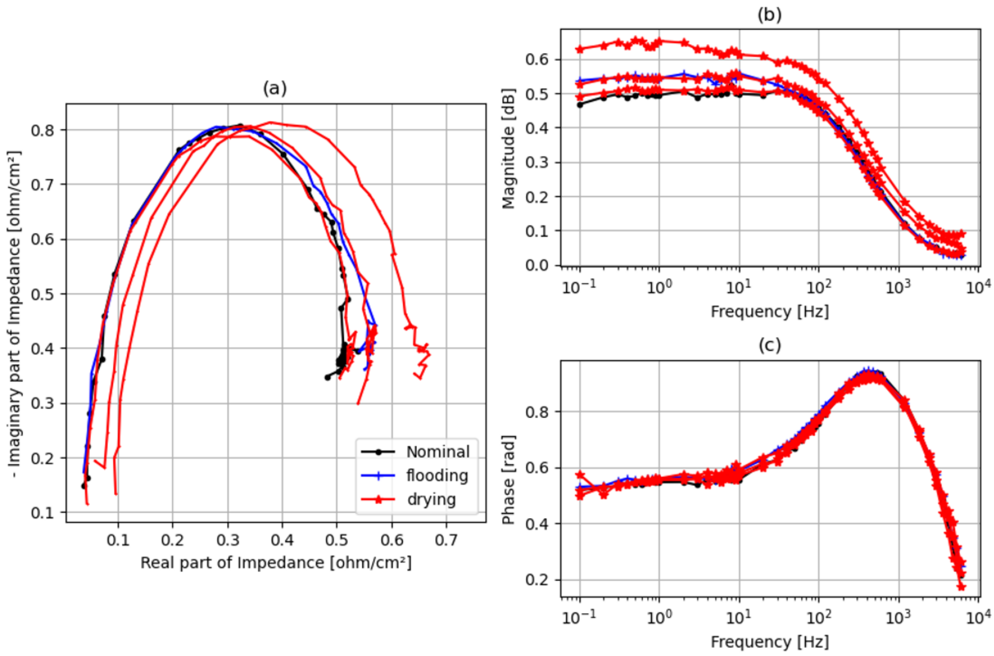

Figure 24 : Comparison of EIS made for H2/O2 stack at 210 Amps in a Nyquist (a) and BODE (b, c) diagrams for nominal, flooding and drying conditions[1]

Figure 25 aims to compare the impacts of starvation at different levels on EIS. For this, three levels of hydrogen and oxygen starvation are tested (low, moderate and high).

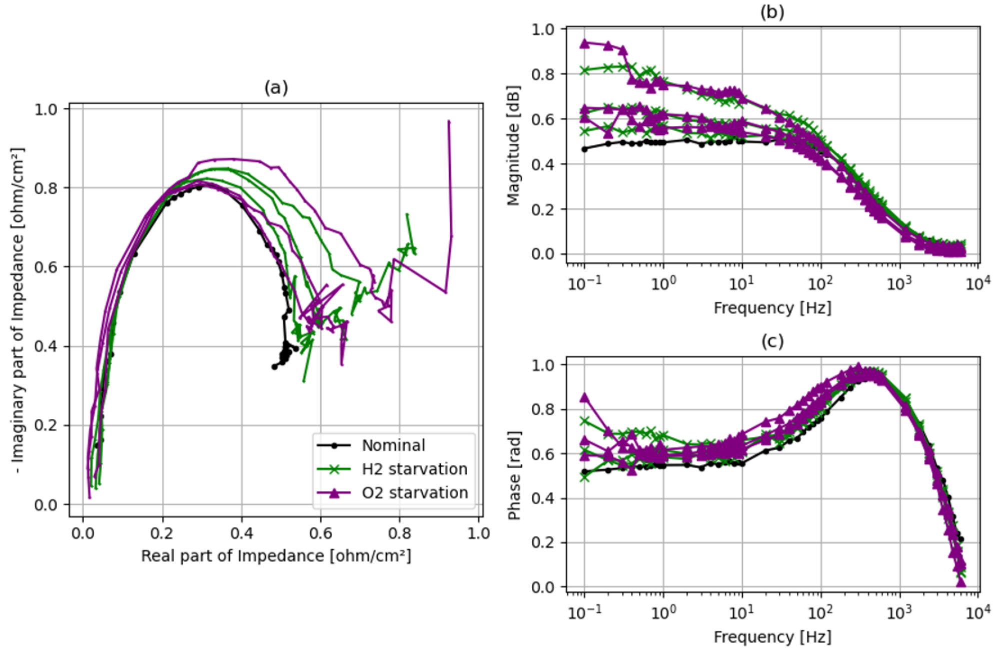

Figure 25 : Comparison of EIS made for H2/O2 stack at 210 Amps in a Nyquist (a) and BODE (b, c) diagrams for nominal and starvation conditions (Oxygen and Hydrogen) [1]

3.4.2 *Presentation of EIS made for H2/AIR stack*

Experimental tests using H2/Air stack were done at 3 current levels but only EIS done at 40 Amps are presented in this section. In each graph an EIS in nominal condition is present to observe the magnitude impact.

[1] Data are normalized for the sake of confidentiality

The Figure 26 in this section represents a comparison between nominal, dry and flood condition in the H2/Air stack. In this configuration, faults levels for flooding and drying represent the anode and cathode side and not an increase of the fault as it is the case for H2/O2 short stack.

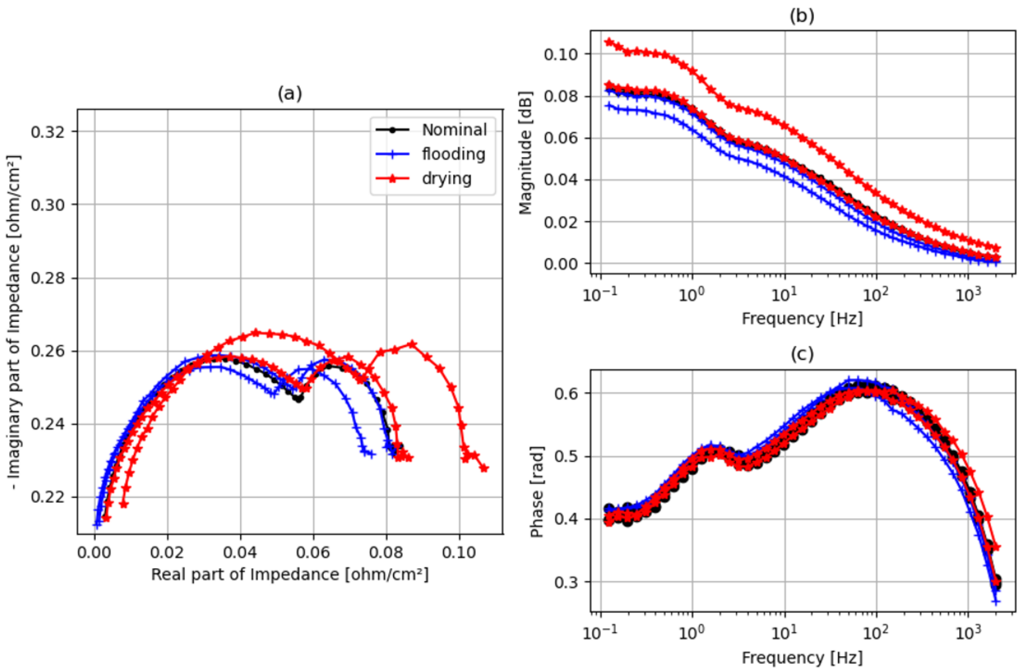

Figure 26 : Comparison in a Nyquist (a) and BODE (b, c) diagrams of EIS made for H2/AIR stack at 40 Amps in nominal, flood and dry conditions [2]

The Figure 27 represents two levels of starvation (Air and Hydrogen). In this configuration the two faults levels which are tested are low and medium starvation.

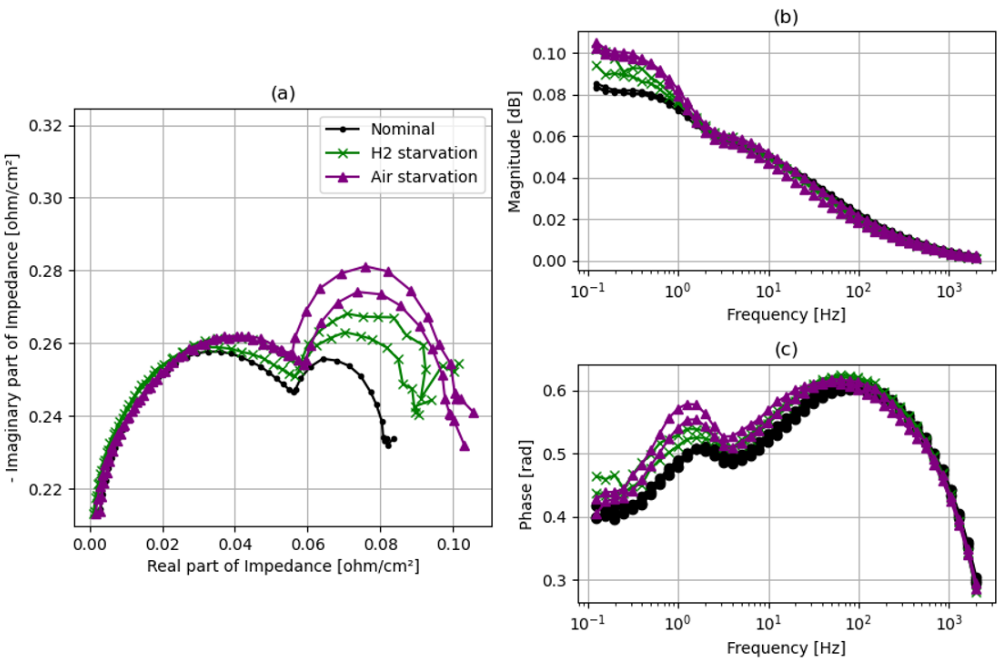

Figure 27 : Comparison in a Nyquist (a) and BODE (b, c) diagrams of EIS made for H2/Air stack at 40 Amps in nominal and starvation (Air & Hydrogen) conditions[2]

The Figure 28 shows the impact of two contaminants (Carbon Monoxide and Sulphur which can appear in case of reformer malfunction. For the case of Carbon Monoxide (CO), several "low" levels of contaminants are tested (4, 6, 8

[2] Data are normalized for the sake of confidentiality

and 12 ppm) and three more levels are tested to represent moderate and high condition of poisoning (80, 120 and 160 ppm). In the configuration where sulfur poisoning is tested, four levels of contamination are tested: 4, 6, 8, 10 ppm. However, unlike CO poisoning, it is impossible to recover the performance lost due to sulfur poisoning. Moreover, sulfur poisoning has a cumulative effect. Therefore, EIS are different from each other in Sulfur Poisoning.

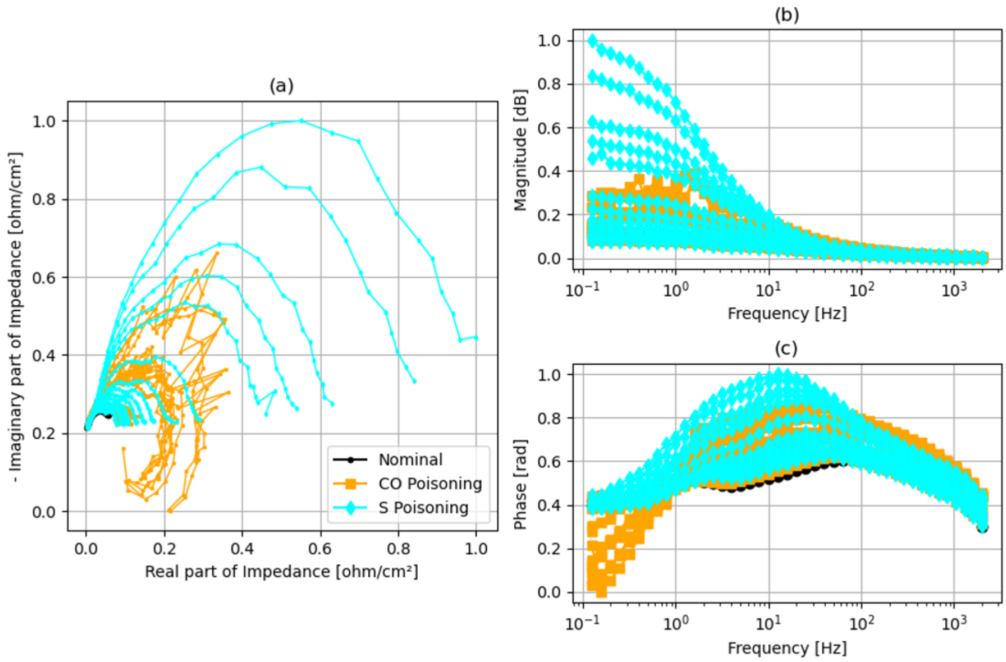

Figure 28 : Comparison in a Nyquist (a) and BODE (b, c) diagrams of EIS made for H2/Air stack at 40 Amps in nominal and poisoned (Carbon Monoxide & Sulphur) conditions[3]

The difference between the composition of reactants in cathode side (Air or O_2) can be analyzed. It is worth observing that the H2/Air technology spectra show two visible arcs that warp up under faulty states. H2/O2 spectra show only one visible arc which shape changes under faulty conditions. Moreover, one can observe a specific change of geometrical shape of the EIS spectrum according to the related operating condition, thus leading to a suitable diagnostic tool implementation.

Another main point visible on these pictures is that poisoning conditions represent a key-feature in the database. Poisoning shows the importance of reactants' composition. A remarkable alteration of the CO poisoning is that at high concentration and constant current density, the imaginary part of EIS becomes positive. This phenomenon is explained in (Wagner and Gülzow, 2004). This characteristic is an important point for diagnostic algorithm as already presented in section 2.2.1.

4 Results and discussion

In this section, the specifications for each dataset and results obtained from the classification are presented. For each of them, a comparison of three features selection methods will be performed in order to validate the selected method.

[3] Data are normalized for the sake of confidentiality

4.1 Specifications for classification

4.1.1 H2/O2 short stack specifications

An important point when using C-Means clustering is the number of clusters as explained in the section 1.3. For both datasets used, the number of clusters corresponds to the number of fault's level tested. Table 5 shows the number of clusters selected for each fault in the H2/O2 dataset:

Table 5 : Number of clusters used for each fault during the classification of H2/O2 dataset

Faults	**Nominal**	**Flooding**	**Drying**	**H_2 Starvation**	**O_2 Starvation**
Clusters' Number	1	1	3	3	3
Fault's level tested	-	-	Low Medium High	Low Medium High	Low Medium High

4.1.2 H2/Air stack specifications

As explained is section 2, H2/Air diagnosis algorithm is composed of two steps of clustering, it is necessary to select for each step the number of clusters corresponding to each class.

For the first step, the objective is to determine if a point is poisoned with carbon monoxide at high concentration or not. So, In the first case one cluster is created with all learning data (before standardization) except the ones with high CO poisoning and another one with all high CO poisoned data.

The Table 6 displays the number of clusters selected for the first step as explained in the paragraph above

Table 6 : Summary of the number cluster chosen for first loop of H2/Air stack diagnosis

Faults	**Carbon monoxide (> 80ppm)**	**All Other Faults**
Clusters' number	1	1

Concerning the second step of algorithm, objective is to classify a data in the right class (i.e. fault). The number of clusters is determined using the number of degradation's level for each fault. Concerning CO poising, degradation's level represent in this second loop are all these inferior to 80 ppm which are not detected in the first loop. Table 7 summarizes the choices done:

Table 7 : Resume of cluster's number chosen for each class during H2/Air second step diagnosis

Faults	**Nominal**	**Flooding**	**Drying**	**H_2 Starvation**	**O_2 Starvation**	**CO poisoning (< 80 ppm)**	**S poisoning**
Clusters' Number	1	2	2	2	2	3	4
Fault's level tested	-	Anode Cathode	Anode Cathode	Low High	Low High	4 ppm 8 ppm 12 ppm	4 ppm 6 ppm 8 ppm 10 ppm

4.2 Cross-Validation Results & features selected analysis

Once all parameters (i.e. Feature Generation) of the algorithm have been determined and the number of clusters for each fault is set the diagnostic procedure can start. Sections 2 and 4.1 detail the different parameters of the algorithm.

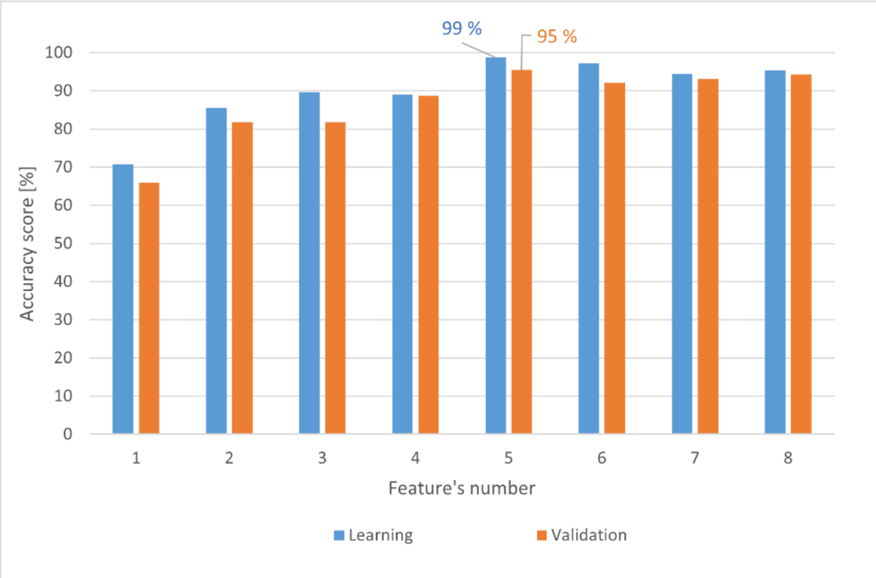

In Figure 29 and Figure 30, the accuracies scores obtained with the Leave One Out methodology are shown.

Figure 29 : Representation of accuracies scores obtained with a leave one out CV test for off and on-line section for H2/O2 stack

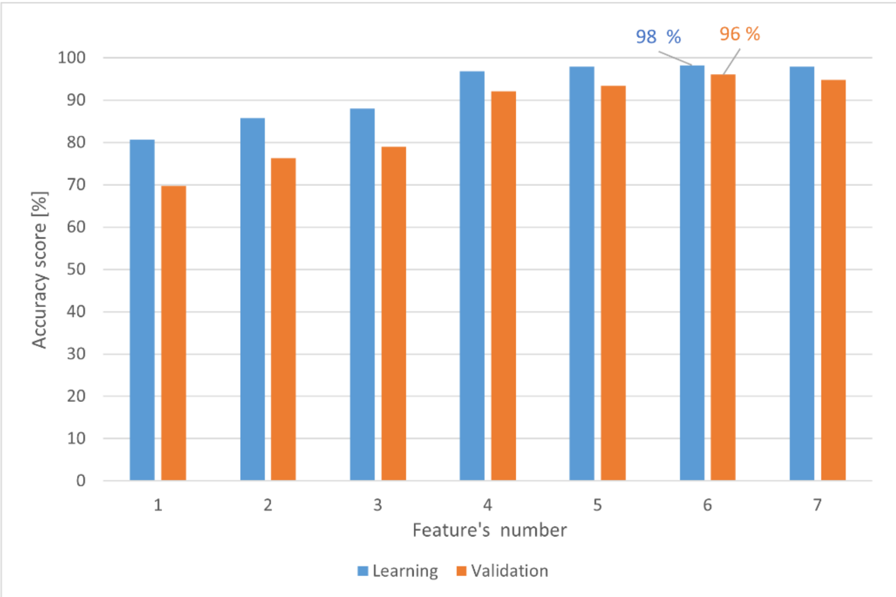

Figure 30 : Representation of accuracies score obtained with a leave one out CV test for off and on-line section for H2/Air stack

Figure 29 shows the best result using cross-validation is obtained using 5 features. Similarly, for the H2/Air stack, the optimum number of features is 6 as Figure 30 shows while the number of faults is increased by two. This proves the efficiency of to isolate in a first step high carbon monoxide poisoned data using imaginary part at low frequency (0.1 Hz) before their standardization.

In the following, the number of features retained is 5 for H2/O2 stack and 6 for H2/Air stack.

Once the number of features has been determined through cross-validation, it is interesting to compare the percentages of selection of each descriptor during the cross-validation phase.

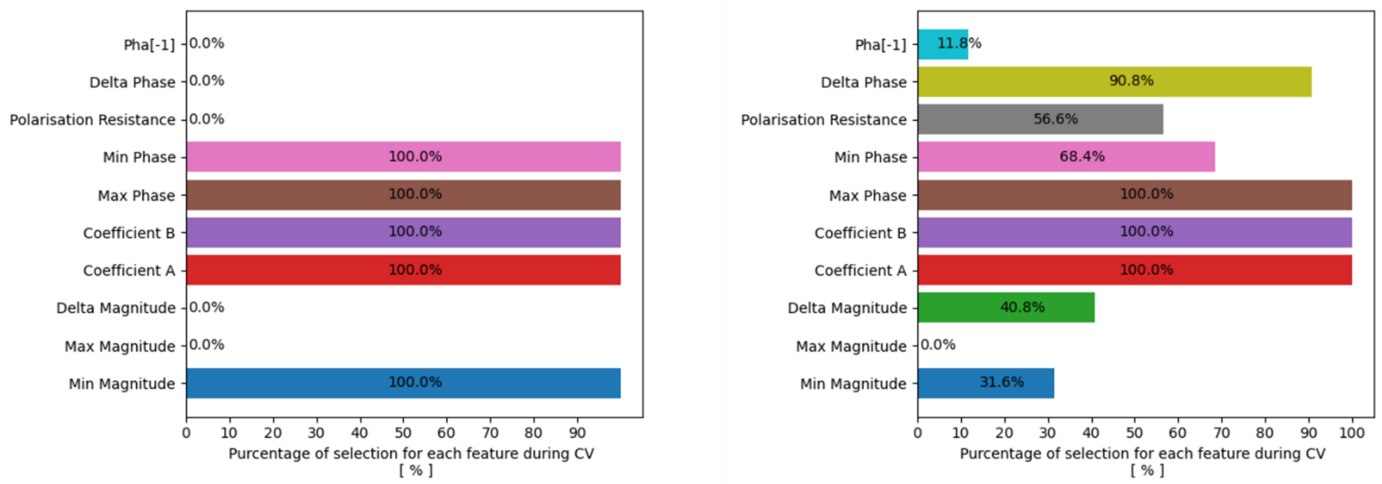

Figure 31 : Representation of the features selected during cross-validation for the H2/O2 (left) and H2/Air (right) stacks

Figure 31 compares the selection rates of each feature during cross-validation for both datasets. It appears that in both datasets, there are three features that are selected for each loop of the cross-validation: *Mp* as well as *Coeff A* and *Coeff B* that come from the analysis of the phase in the range [10, 1] Hz.

This similarity between the two datasets allows us to assess that these three features correctly represent the faults related to starvation and water management since they are present in both databases. This can be explained because these features give information about the charge transfer of oxygen reduction reaction which occur in the range [1 – 10^3] Hz and are the main effect of these faults as described in section 3.1.

In the case of H2/O2 stack, in addition to the three features described above, the same other features are always selected (i.e. *mp* and *mm*), whereas in the case of H2/Air technology, depending on the data tested, the features selected may vary greatly. Minimal magnitude and minimal phase give information on the transfer charge of hydrogen oxidation reaction but also, minimal magnitude corresponds to the ohmic resistance which is highly impacted as shown in experimental section.

The variation of features selected during cross-validation for H2/Air stack may be due to the influence of a data in relation between features and the global variance of a feature. Indeed, in H2/O2 short stack, as section 3.4 shows, EIS are similar and in the same scale which is not the case in H2/Air stack due to the presence of poisoning faults. Therefore, variance and correlation between features in the short-stack dataset are more "stable" and less impact with the rotation of validation data during cross-validation step than H2/Air technology.

However, one can still notice that the most frequently selected descriptors in the H2/Air database are: *Mp*, *Coeff B*, *Coeff A*, *ΔPha*, *mp* and *R_Pola*. In the case where it would be necessary to switch from an automatic selection of descriptors to a pre-defined selection, these 6 descriptors would allow a better characterization of this dataset. This selection allows representing each fault: as explained in previous paragraph, *Mp*, *Coeff B*, *Coeff A* and *mp* give an overview on starvation and water management faults while *ΔPha*, and *R_Pola* give information about diffusion phenomena in the FC which is directly linked to poisoning faults.

Another interesting point is the fact that for both stacks, the maximum magnitude (Mm) is never selected. Given that the minimum amplitude and the difference between the two magnitudes are filled in. This "not selection" can be explained because of all EIS used in this paper are complete while the maximal magnitude mainly used for uncomplete spectra.

4.3 Analysis of results

As presented in section 2.4 confusion matrices are one of the most widely used tools for analyzing classification results. Figure 32 shows the confusion matrix for the datasets using the LOO method with fuzzy C-means clustering present in the previous section.

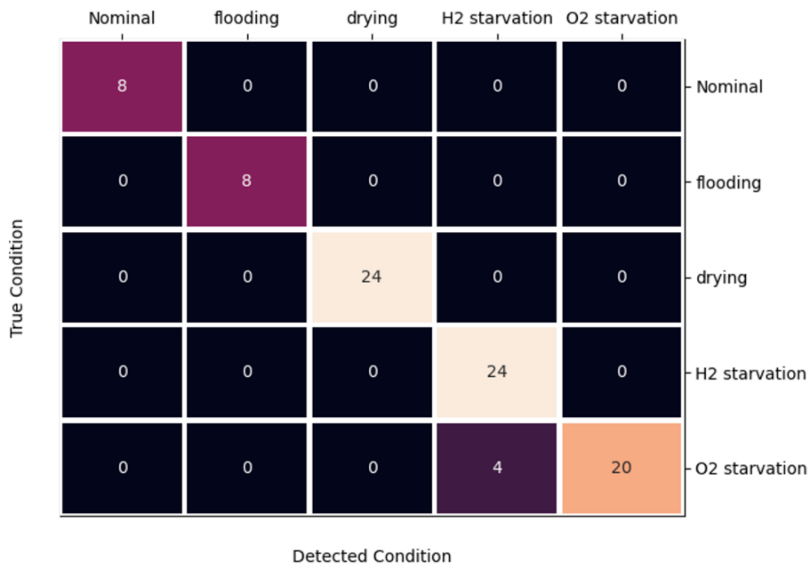

Figure 32: Validation Confusion Matrix for the H2/O2 dataset with 5 features selected

As Figure 32 shows, classification algorithm is very powerful, all faults are correctly detected except for 4 confusions between oxygen and hydrogen starvation. This confusion can be explained because hydrogen starvation and oxygen starvation are two very similar failures.

Figure 33 represents the confusion matrix for the H2/Air diagnosis algorithm.

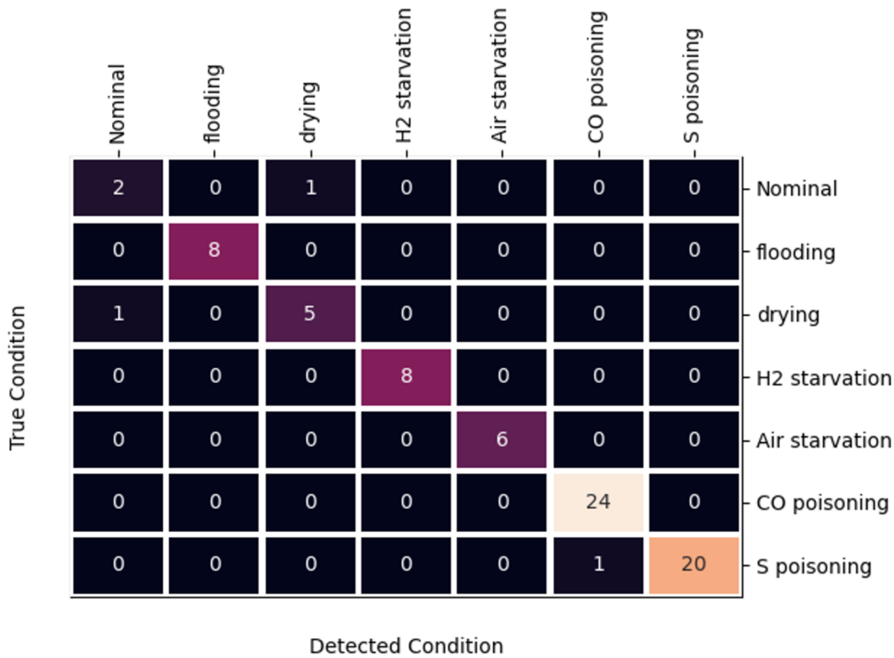

Figure 33: Confusion matrix for H2/Air diagnosis using 6 features

In the same way as for the H2/O2 stack, Figure 33 shows that the algorithm is efficient to properly detect and classify most data.

In the end, only three data were misclassified: two inversions between flooding and drying of the stack and one inversion between carbon monoxide poisoning and sulfur poisoning. The confusion between the nominal operation and the drying up may be because only three EIS in nominal operation have been entered in the algorithm, which is highly insufficient to create good quality clusters.

In addition to this reduced amount of data, the fact that the faults tested for the stack are so-called "emerging" faults (i.e. incipient or very low intensity faults) complicates the detection task. Indeed, emerging faults are very closed to nominal conditions. Emerging faults may also explain the confusion between carbon monoxide and sulfur poisoning since the only range in which these faults can be confused is that of low intensity faults (< 80ppm).

4.4 Evaluation of the algorithm performances

4.4.1 Influence of the selection step

Since feature selection is one of the key steps of Machine Learning, a comparison between the method used in this article and two others is presented in this section.

The first one is based solely on PCC to eliminate redundant information and the selected features are then sorted according to their variance. The second one uses the ANOVA F-Test to sort the features. The last is the method used in this paper: a combination between both methods where features are filtered using PCC and then sort with ANOVA F-Test. The purpose of this comparison is to prove the usefulness of combining both filtering and statistical testing in order to optimize the results.

Table 8 compares the validation results (using a LOO Cross validation methodology) between the three types of features selection for each stack using a Quantile Transformer standardization method:

Table 8 : Comparison between several Feature Selection methodology for both datasets

	PCC		**ANOVA F-Test**		**PCC + ANOVA F-Test**	
Features' number	*Accuracy score [%]*		*Accuracy score [%]*		*Accuracy score [%]*	
	H2/O2	**H2/Air**	**H2/O2**	**H2/Air**	**H2/O2**	**H2/Air**
1	61	61	66	70	66	70
2	58	72	82	72	82	76
3	60	91	82	78	82	79
4	73	92	88	91	89	92
5	81	89	84	92	**95**	93
6	90	91	**94**	95	92	**96**
7	93	**95**	91	**95**	93	95
8	**94**	89	93	95	94	89
9	x	x	93	95	x	x
10	x	x	93	89	x	x

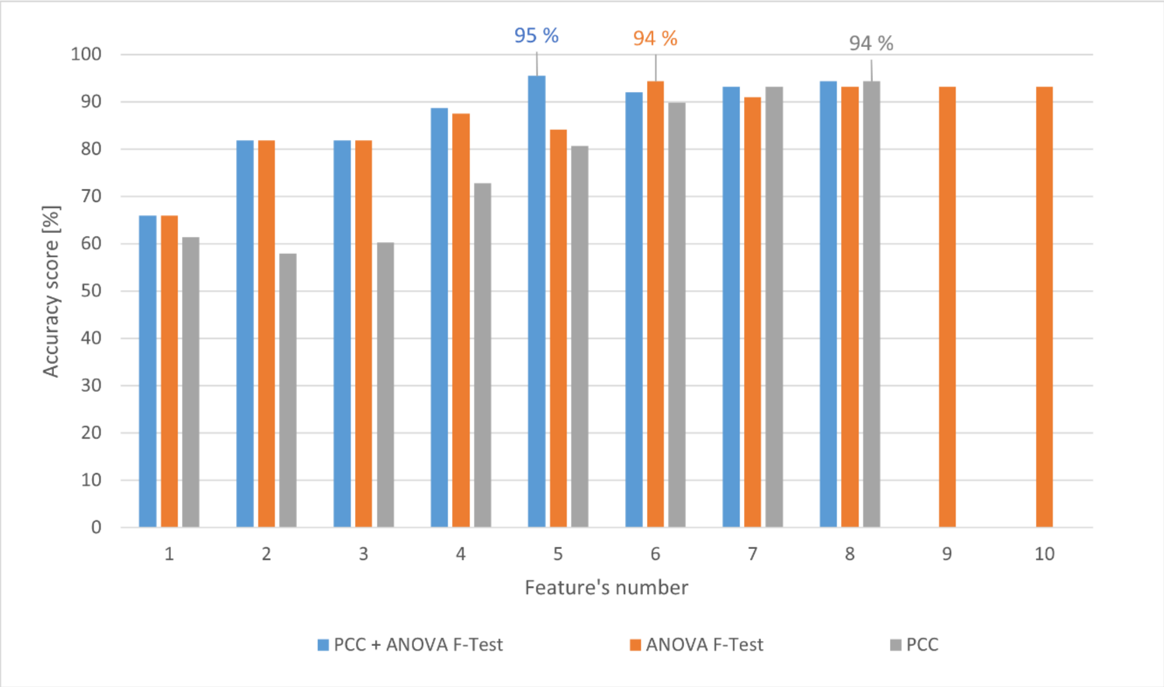

Figure 34 : Presentation of accuracy score obtained with several feature selection methods for H2/O2 stack

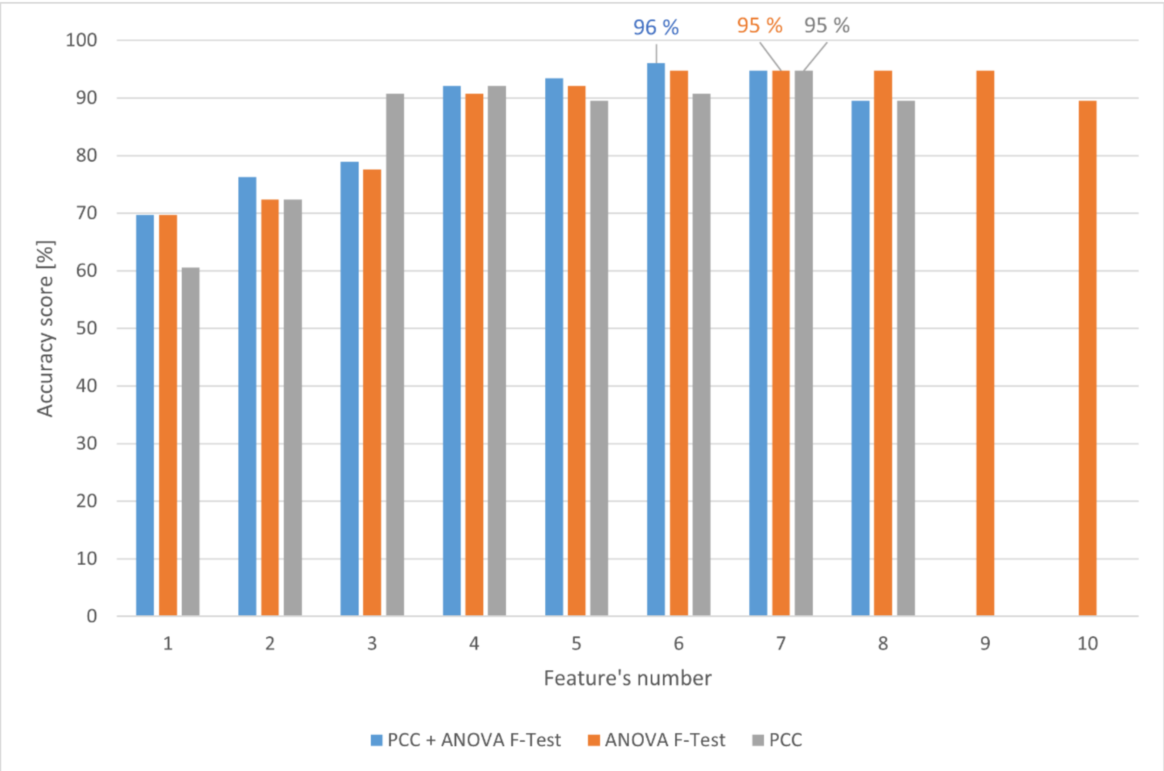

Figure 35 : Presentation of accuracy score obtain with several feature selection methods for H2/Air stack

As Figure 34 and Figure 35 shown, the combination of PCC and ANOVA F-Test increases the accuracy of results and in the case of H2/O2 dataset it reduces the number of features to select. In addition to increase result, a good selection of features increases the robustness of the algorithm. Indeed, the robustness can be affected when using Fuzzy C-means methods because of the presence of local optima during cluster creation. To obtain a good robustness it is necessary to select the right features, but the standardization methods are also to be considered in the case of algorithms based on distances to classify the data.

In most cases increasing the number of features increases the accuracy of algorithm until reaching a limit number of features from which the results fall. Too many features may be a sign of the overfitting phenomenon. This phenomenon can be seen in Figure 34 and Figure 35 however, there is an exception in the H2/air dataset. When features are filtered with PCC and sort by their variance there is a local optimum at 5 features which shows a weakness in the method. This shows that the variance criterion is insufficient to classify features. Regarding the results, it appears that sort features by variance is less efficient that sort them using the ANOVA F-Test.

According to results, the best methods is the combination of PCC and ANOVA F-Test which permits to reduce the number of features and increase accuracy results of algorithm.

Conclusion

Diagnosis is a crucial tool for the prolongation of fuel cell lifetime. In this paper, a non model-based method is proposed to detect and identify several faults in fuel cells. The strength of the algorithm lies in the way it generates the features. Indeed, it extracts a set of features from EIS spectra, then uses a quantum-based standardization method to limit the impact of outliers and finally selects the best features by filtering out redundancies before applying a statistical test. To classify data, it uses a Fuzzy C-means clustering algorithm. The combination of feature generation and Fuzzy C-means classifier provides a simple algorithm that does not require a lot of machine learning skills. However, despite its simplicity, the method presented is robust and not very sensitive to noisy data.

In order to validate this algorithm, tests have been performed on two different stacks to obtain two databases. The tests have not been performed in the same infrastructure and under the same conditions. As each basis suffers from unavoidable biases and as they concern different technologies and measurements are carried out on different test benches, there is no chance that these biases are the same. Nevertheless, the diagnostic algorithm was able to provide classification results of about 95% during the cross-validation. This proves that despite the differences between the data (stack technologies, cathode gas, noise, faults tested, measurement biases, ...), the algorithm is quite capable of detecting abnormal operating conditions and therefore there is a generality of the method. Furthermore, the most frequently encountered faults are taken into account and handled by the algorithm.

In addition, for both technologies the features selected were analyzed to observe the link between the selection done by the algorithm and the physical phenomena. It appears that according to the faults tested, the algorithm selects only those features that correspond to the frequency range in which the faults are visible. However, the number of features is important and must be chosen carefully to avoid a spatial dimension that favors one fault over the others. The algorithm is then able to operate in an automatic way, without expertise of the user, once the database is set.

In this paper, a short comparison between some methods for selecting descriptors is proposed. However, it would be interesting to develop it to also observe the impact of the standardization method on robustness and precision. These steps have been performed during the development of the method but are not presented in this document.

Acknowledgments

This work has been supported by the EIPHI Graduate School (contract ANR-17- EURE-0002) and the Region Bourgogne Franche-Comté.

The research leading to these results has received funding from the European Union's Horizon2020 Program (2020-JTI-FCH-2014-1) for the Fuel Cells and Hydrogen Joint Undertaking, under grant agreement number 671486 – Research and Innovation Project: HEALTH-CODE (Real operation pem fuel cells HEALTH-state monitoring and diagnosis based on dc-dc Converter embeddeD Eis). Website: http://pemfc. health-code.eu/

This project has received funding from the Fuel Cells and Hydrogen 2 Joint Undertaking (JU) under grant agreement No 875047. The JU receives support from the European Union's Horizon 2020 research and innovation programme and Italy, France, Denmark, Slovenia, Finland, Germany, Switzerland. Website : https://www.rubyproject.eu/

References

Bernardi, D.M., Verbrugge, M.W., 1991. Mathematical model of a gas diffusion electrode bonded to a polymer electrolyte. AIChE J. 37, 1151–1163. https://doi.org/10.1002/aic.690370805

Bressel, M., Hilairet, M., Hissel, D., Ould Bouamama, B., 2016. Extended Kalman Filter for prognostic of Proton Exchange Membrane Fuel Cell. Appl. Energy 164, 220–227. https://doi.org/10.1016/j.apenergy.2015.11.071

Cadet, C., Jemeï, S., Druart, F., Hissel, D., 2014. Diagnostic tools for PEMFCs: from conception to implementation. Int. J. Hydrog. Energy 39, 10613–10626. https://doi.org/10.1016/j.ijhydene.2014.04.163

Chen, J., Zhou, B., 2008. Diagnosis of PEM fuel cell stack dynamic behaviors. J. Power Sources 177, 83–95. https://doi.org/10.1016/j.jpowsour.2007.11.038

Chok, N.S., 2010. PEARSON'S VERSUS SPEARMAN'S AND KENDALL'S CORRELATION COEFFICIENTS FOR CONTINUOUS DATA.

De Lira, S., Puig, V., Quevedo, J., 2009. LPV Model-Based Fault Diagnosis Using Relative Fault Sensitivity Signature Approach in a PEM Fuel Cell. IFAC Proc. Vol., 7th IFAC Symposium on Fault Detection, Supervision and Safety of Technical Processes 42, 528–533. https://doi.org/10.3182/20090630-4-ES-2003.00088

Ding, S.X., 2008. Model-based Fault Diagnosis Techniques. Springer Berlin Heidelberg, Berlin, Heidelberg. https://doi.org/10.1007/978-3-540-76304-8

Escobet, A., Nebot, À., Mugica, F., 2014. PEM fuel cell fault diagnosis via a hybrid methodology based on fuzzy and pattern recognition techniques. Eng. Appl. Artif. Intell. 36, 40–53. https://doi.org/10.1016/j.engappai.2014.07.008

Farrell, C.G., Gardner, C.L., Ternan, M., 2007. Experimental and modelling studies of CO poisoning in PEM fuel cells. J. Power Sources 171, 282–293. https://doi.org/10.1016/j.jpowsour.2007.07.006

Fouquet, N., Doulet, C., Nouillant, C., Dauphin-Tanguy, G., Ould-Bouamama, B., 2006. Model based PEM fuel cell state-of-health monitoring via ac impedance measurements. J. Power Sources 159, 905–913. https://doi.org/10.1016/j.jpowsour.2005.11.035

Fuel Cells [WWW Document], n.d. . Energy.gov. URL https://www.energy.gov/eere/fuelcells/fuel-cells (accessed 1.17.21).

Gharavian, M.H., Almas Ganj, F., Ohadi, A.R., Heidari Bafroui, H., 2013. Comparison of FDA-based and PCA-based features in fault diagnosis of automobile gearboxes. Neurocomputing 121, 150–159. https://doi.org/10.1016/j.neucom.2013.04.033

Giurgea, S., Tirnovan, R., Hissel, D., Outbib, R., 2013. An analysis of fluidic voltage statistical correlation for a diagnosis of PEM fuel cell flooding. Int. J. Hydrog. Energy 38, 4689–4696. https://doi.org/10.1016/j.ijhydene.2013.01.060

Hamaz, T., 2014. Outils de caractérisation et de diagnostic d'une pile à combustible de type PEM par mesure du champ électromagnétique externe. Université de Grenoble.

Hickner, M.A., Fujimoto, C.H., Cornelius, C.J., 2006. Transport in sulfonated poly(phenylene)s: Proton conductivity, permeability, and the state of water. Polymer 47, 4238–4244. https://doi.org/10.1016/j.polymer.2006.02.034

Hinaje, M., Sadli, I., Martin, J.-P., Thounthong, P., Raël, S., Davat, B., 2009. Online humidification diagnosis of a PEMFC using a static DC–DC converter. Int. J. Hydrog. Energy 34, 2718–2723. https://doi.org/10.1016/j.ijhydene.2009.01.076

Hissel, D., Péra, M.C., Kauffmann, J.M., 2004. Diagnosis of automotive fuel cell power generators. J. Power Sources 128, 239–246. https://doi.org/10.1016/j.jpowsour.2003.10.001

HJ, 2019. Hydrogen [WWW Document]. Energy - Eur. Comm. URL https://ec.europa.eu/energy/topics/energy-system-integration/hydrogen_en (accessed 1.11.21).

Jayaraj, P., Karthika, P., Rajalakshmi, N., Dhathathreyan, K.S., 2014. Mitigation studies of sulfur contaminated electrodes for PEMFC. Int. J. Hydrog. Energy 39, 12045–12051. https://doi.org/10.1016/j.ijhydene.2014.06.011

Jemeï, S., Hissel, D., Péra, M.C., Kauffmann, J.M., 2003. On-board fuel cell power supply modeling on the basis of neural network methodology. J. Power Sources 124, 479–486. https://doi.org/10.1016/S0378-7753(03)00799-7

Johnson, K.J., Synovec, R.E., 2002. Pattern recognition of jet fuels: comprehensive GC×GC with ANOVA-based feature selection and principal component analysis. Chemom. Intell. Lab. Syst., Fourth International Conference on Environ metrics and Chemometrics held in Las Vegas, NV, USA, 18-20 September 2000 60, 225–237. https://doi.org/10.1016/S0169-7439(01)00198-8

Josh Warner, Jason Sexauer, scikit-fuzzy, twmeggs, alexsavio, Aishwarya Unnikrishnan, Guilherme Castelão, Felipe Arruda Pontes, Tobias Uelwer, pd2f, laurazh, Fernando Batista, alexbuy, Wouter Van den Broeck, William Song, The Gitter Badger, Roberto Abdelkader Martínez Pérez, James F. Power, Himanshu Mishra, Guillem Orellana Trullols, Axel Hörteborn, 99991, 2019. JDWarner/scikit-fuzzy: Scikit-Fuzzy version 0.4.2. Zenodo. https://doi.org/10.5281/zenodo.3541386

Kaid, I.E., Hafaifa, A., Guemana, M., Hadroug, N., Kouzou, A., Mazouz, L., 2018. Photovoltaic system failure diagnosis based on adaptive neuro fuzzy inference approach: South Algeria solar power plant. J. Clean. Prod. 204, 169–182. https://doi.org/10.1016/j.jclepro.2018.09.023

Kim, J., Lee, I., Tak, Y., Cho, B.H., 2012. State-of-health diagnosis based on hamming neural network using output voltage pattern recognition for a PEM fuel cell. Int. J. Hydrog. Energy 37, 4280–4289. https://doi.org/10.1016/j.ijhydene.2011.11.092

Li, H., Tang, Y., Wang, Z., Shi, Z., Wu, S., Song, D., Zhang, Jianlu, Fatih, K., Zhang, Jiujun, Wang, H., Liu, Z., Abouatallah, R., Mazza, A., 2008. A review of water flooding issues in the proton exchange membrane fuel cell. J. Power Sources 178, 103–117. https://doi.org/10.1016/j.jpowsour.2007.12.068

Li, Z., 2014. Data-driven fault diagnosis for PEMFC systems. UNIVERSITE D'AIXMARSEILLE,.

Li, Z., Outbib, R., Giurgea, S., Hissel, D., Jemei, S., Giraud, A., Rosini, S., 2016. Online implementation of SVM based fault diagnosis strategy for PEMFC systems. Appl. Energy 164, 284–293. https://doi.org/10.1016/j.apenergy.2015.11.060

Lin, R.-H., Xi, X.-N., Wang, P.-N., Wu, B.-D., Tian, S.-M., 2019. Review on hydrogen fuel cell condition monitoring and prediction methods. Int. J. Hydrog. Energy 44, 5488–5498. https://doi.org/10.1016/j.ijhydene.2018.09.085

Liu, H., Liu, L., Zhang, H., 2008. Feature Selection Using Mutual Information: An Experimental Study, in: Ho, T.-B., Zhou, Z.-H. (Eds.), PRICAI 2008: Trends in Artificial Intelligence, Lecture Notes in Computer Science. Springer Berlin Heidelberg, Berlin, Heidelberg, pp. 235–246. https://doi.org/10.1007/978-3-540-89197-0_24

Liu, J., Li, Q., Chen, W., Cao, T., 2018. A discrete hidden Markov model fault diagnosis strategy based on K-means clustering dedicated to PEM fuel cell systems of tramways. Int. J. Hydrog. Energy 43, 12428–12441. https://doi.org/10.1016/j.ijhydene.2018.04.163

Liu, J., Luo, W., Yang, X., Wu, L., 2016. Robust Model-Based Fault Diagnosis for PEM Fuel Cell Air-Feed System. IEEE Trans. Ind. Electron. 63, 3261–3270. https://doi.org/10.1109/TIE.2016.2535118

Lopes, T., Paganin, V.A., Gonzalez, E.R., 2011. The effects of hydrogen sulfide on the polymer electrolyte membrane fuel cell anode catalyst: H2S–Pt/C interaction products. J. Power Sources 196, 6256–6263. https://doi.org/10.1016/j.jpowsour.2011.04.017

Medjahed, S.A., Saadi, T., Benyettou, A., 2013. Breast Cancer Diagnosis by using k-Nearest Neighbor with Different Distances and Classification Rules. Int. J. Comput. Appl. 62, 1–5. https://doi.org/10.5120/10041-4635

Mennola, T., Mikkola, M., Noponen, M., Hottinen, T., Lund, P., 2002. Measurement of ohmic voltage losses in individual cells of a PEMFC stack. J. Power Sources 112, 261–272. https://doi.org/10.1016/S0378-7753(02)00391-9

Mérida, W., Harrington, D.A., Le Canut, J.M., McLean, G., 2006. Characterisation of proton exchange membrane fuel cell (PEMFC) failures via electrochemical impedance spectroscopy. J. Power Sources 161, 264–274. https://doi.org/10.1016/j.jpowsour.2006.03.067

Mohsin, M., Raza, R., Mohsin-ul-Mulk, M., Yousaf, A., Hacker, V., 2020. Electrochemical characterization of polymer electrolyte membrane fuel cells and polarization curve analysis. Int. J. Hydrog. Energy 45, 24093–24107. https://doi.org/10.1016/j.ijhydene.2019.08.246

Mouzakitis, A., 2013. Classification of Fault Diagnosis Methods for Control Systems. Meas. Control 46, 303–308. https://doi.org/10.1177/0020294013510471

Pahon, E., Yousfi Steiner, N., Jemei, S., Hissel, D., Moçoteguy, P., 2016. A signal-based method for fast PEMFC diagnosis. Appl. Energy 165, 748–758. https://doi.org/10.1016/j.apenergy.2015.12.084

Pedregosa, F., Varoquaux, G., Gramfort, A., Michel, V., Thirion, B., Grisel, O., Blondel, M., Prettenhofer, P., Weiss, R., Dubourg, V., Vanderplas, J., Passos, A., Cournapeau, D., Brucher, M., Perrot, M., Duchesnay, É., 2011. Scikit-learn: Machine Learning in Python. J. Mach. Learn. Res. 12, 2825–2830.

Pei, P., Wu, Z., Li, Y., Jia, X., Chen, D., Huang, S., 2018. Improved methods to measure hydrogen crossover current in proton exchange membrane fuel cell. Appl. Energy 215, 338–347. https://doi.org/10.1016/j.apenergy.2018.02.002

Petrone, R., Vitagliano, C., Péra, M.-C., Chamagne, D., Sorrentino, M., 2018. Characterization of an H_2/O_2 PEMFC Short-Stack Performance Aimed to Health-State Monitoring and Diagnosis. Fuel Cells 18, 279–286. https://doi.org/10.1002/fuce.201700112

Petrone, R., Zheng, Z., Hissel, D., Péra, M.C., Pianese, C., Sorrentino, M., Becherif, M., Yousfi-Steiner, N., 2013. A review on model-based diagnosis methodologies for PEMFCs. Int. J. Hydrog. Energy 38, 7077–7091. https://doi.org/10.1016/j.ijhydene.2013.03.106

Rafiee, J., Tse, P.W., 2009. Use of autocorrelation of wavelet coefficients for fault diagnosis. Mech. Syst. Signal Process. 23, 1554–1572. https://doi.org/10.1016/j.ymssp.2009.02.008

Real operation pem fuel cells HEALTH-state monitoring and diagnosis based on dc-dc COnverter embeddeD Eis [WWW Document], n.d. URL https://pemfc.health-code.eu/ (accessed 12.29.20).

Real operation pem fuel cells HEALTH-state monitoring and diagnosis based on dc-dc COnverter embeddeD Eis;H2020, European project, Horizon 2020; Health-Code [WWW Document], n.d. URL http://pemfc.health-code.eu/ (accessed 8.23.20).

Riascos, L.A.M., Simoes, M.G., Miyagi, P.E., 2007. A Bayesian network fault diagnostic system for proton exchange membrane fuel cells. J. Power Sources 165, 267–278. https://doi.org/10.1016/j.jpowsour.2006.12.003

Rubio, M.A., Urquia, A., Dormido, S., 2007. Diagnosis of PEM fuel cells through current interruption. J. Power Sources 171, 670–677. https://doi.org/10.1016/j.jpowsour.2007.06.072

RUBY – EU project, n.d. URL https://www.rubyproject.eu/ (accessed 2.2.21).

Sanchez, R.E.S., 2015. Contribution au pronostic de durée de vie des systèmes piles à combustible PEMFC. Université de Franche-Comté,.

Schmittinger, W., Vahidi, A., 2008. A review of the main parameters influencing long-term performance and durability of PEM fuel cells. J. Power Sources 180, 1–14. https://doi.org/10.1016/j.jpowsour.2008.01.070

Sethuraman, V.A., Weidner, J.W., 2010. Analysis of sulfur poisoning on a PEM fuel cell electrode. Electrochimica Acta 55, 5683–5694. https://doi.org/10.1016/j.electacta.2010.05.004

Shaikh, R., 2018. Cross Validation Explained: Evaluating estimator performance. [WWW Document]. Medium. URL https://towardsdatascience.com/cross-validation-explained-evaluating-estimator-performance-e51e5430ff85 (accessed 8.26.20).

Shi, W., Yi, B., Hou, M., Jing, F., Ming, P., 2007. Hydrogen sulfide poisoning and recovery of PEMFC Pt-anodes. J. Power Sources 165, 814–818. https://doi.org/10.1016/j.jpowsour.2006.12.052

Taniguchi, A., Akita, T., Yasuda, K., Miyazaki, Y., 2008. Analysis of degradation in PEMFC caused by cell reversal during air starvation. Int. J. Hydrog. Energy 33, 2323–2329. https://doi.org/10.1016/j.ijhydene.2008.02.049

The Future of Hydrogen – Analysis [WWW Document], n.d. . IEA. URL https://www.iea.org/reports/the-future-of-hydrogen (accessed 12.30.20).

Wagner, N., Friedrich, K.A., 2009. FUEL CELLS – PROTON-EXCHANGE MEMBRANE FUEL CELLS | Dynamic Operational Conditions, in: Garche, J. (Ed.), Encyclopedia of Electrochemical Power Sources. Elsevier, Amsterdam, pp. 912–930. https://doi.org/10.1016/B978-044452745-5.00239-2

Wagner, N., Gülzow, E., 2004. Change of electrochemical impedance spectra (EIS) with time during CO-poisoning of the Pt-anode in a membrane fuel cell. J. Power Sources 7.

Wang, H., n.d. PEM Fuel Cell Diagnostic Tools 556.

Wang, H., Macomber, C., Christ, J., Bender, G., Pivovar, B., Dinh, H.N., 2014. Evaluating the Influence of PEMFC System Contaminants on the Performance of Pt Catalyst via Cyclic Voltammetry. Electrocatalysis 5, 62–67. https://doi.org/10.1007/s12678-013-0159-9

Wang, H., Yuan, X.-Z., Li, H., 2012. PEM Fuel Cell Diagnostic Tools.

Yakub, S., Arowolo, M., Abdulsalam, S., M.D., S., 2016. A Feature Selection Based on One Way Anova For Microarray Data Classification 30–35.

Yousfi-Steiner, N., Moçotéguy, Ph., Candusso, D., Hissel, D., 2009. A review on polymer electrolyte membrane fuel cell catalyst degradation and starvation issues: Causes, consequences and diagnostic for mitigation. J. Power Sources 194, 130–145. https://doi.org/10.1016/j.jpowsour.2009.03.060

Yousfi-Steiner, N., Moçotéguy, Ph., Candusso, D., Hissel, D., Hernandez, A., Aslanides, A., 2008. A review on PEM voltage degradation associated with water management: Impacts, influent factors and characterization. J. Power Sources 183, 260–274. https://doi.org/10.1016/j.jpowsour.2008.04.037

Yu, F.T.S., Lu, G., 1994. Short-time Fourier transform and wavelet transform with Fourier-domain processing. Appl. Opt. 33, 5262. https://doi.org/10.1364/AO.33.005262

Yuan, H., Dai, H., Wei, X., Ming, P., 2020. A novel model-based internal state observer of a fuel cell system for electric vehicles using improved Kalman filter approach. Appl. Energy 268, 115009. https://doi.org/10.1016/j.apenergy.2020.115009

Zhang, S., Yuan, X.-Z., Hin, J.N.C., Wang, H., Friedrich, K.A., Schulze, M., 2009. A review of platinum-based catalyst layer degradation in proton exchange membrane fuel cells. J. Power Sources 194, 588–600. https://doi.org/10.1016/j.jpowsour.2009.06.073

Zhao, X., Xu, L., Li, J., Fang, C., Ouyang, M., 2017. Faults diagnosis for PEM fuel cell system based on multi-sensor signals and principle component analysis method. Int. J. Hydrog. Energy 42, 18524–18531. https://doi.org/10.1016/j.ijhydene.2017.04.146

Zhao, Y., Mao, Y., Zhang, W., Tang, Y., Wang, P., 2020. Reviews on the effects of contaminations and research methodologies for PEMFC. Int. J. Hydrog. Energy 45, 23174–23200. https://doi.org/10.1016/j.ijhydene.2020.06.145

Zheng, Z., Morando, S., Pera, M.-C., Hissel, D., Larger, L., Martinenghi, R., Baylon Fuentes, A., 2017. Brain-inspired computational paradigm dedicated to fault diagnosis of PEM fuel cell stack. Int. J. Hydrog. Energy 42, 5410–5425. https://doi.org/10.1016/j.ijhydene.2016.11.043

Zheng, Z., Péra, M.-C., Hissel, D., Becherif, M., Agbli, K.-S., Li, Y., 2014. A double-fuzzy diagnostic methodology dedicated to online fault diagnosis of proton exchange membrane fuel cell stacks. J. Power Sources 271, 570–581. https://doi.org/10.1016/j.jpowsour.2014.07.157

Zheng, Z., Petrone, R., Péra, M.C., Hissel, D., Becherif, M., Pianese, C., Yousfi Steiner, N., Sorrentino, M., 2013. A review on non-model based diagnosis methodologies for PEM fuel cell stacks and systems. Int. J. Hydrog. Energy 38, 8914–8926. https://doi.org/10.1016/j.ijhydene.2013.04.007